Chemical and Spectroscopic Definition of the Peroxide-Level Intermediate in the Multicopper Oxidases: Relevance to the Catalytic Mechanism of Dioxygen Reduction to Water

Woonsup Shin,[†] Uma M. Sundaram,[†] James L. Cole,[†] Hua H. Zhang,[†] Britt Hedman,[‡] Keith O. Hodgson,[†,‡] and Edward I. Solomon*[,†]

Contribution from the Department of Chemistry, Stanford University and Stanford Synchrotron Radiation Laboratory, Stanford, California 94305

Received October 30, 1995[⊗]

Abstract: Laccase is a multicopper oxidase which contains four coppers, one type 1, one type 2, and a coupled binuclear type 3 pair, the type 2 and type 3 copper centers together forming a trinuclear copper cluster. The type 1 mercury derivative of laccase (T1Hg Lc) has the type 1 center substituted with a redox inactive Hg^{2+} ion and an intact trinuclear copper cluster. Reaction of reduced T1Hg Lc with dioxygen produces an oxygen intermediate which has now been studied in detail. Isotope ratio mass spectrometry (IRMS) has shown that both oxygen atoms of O_2 are bound in the intermediate. EPR and SQUID magnetic susceptibility studies have shown that the intermediate is diamagnetic. The results combined with X-ray absorption edge data indicate that the intermediate contains a bound peroxide and that the two electrons have derived from the type 3 center which is antiferromagnetically coupled. EXAFS data show that there is no short Cu−oxo bond in the intermediate and that there is a new bridging interaction in the intermediate, with two coppers being separated by 3.4 Å, that is not present in the resting enzyme. Circular dichroism (CD) and magnetic circular dichroism (MCD) studies in the ligand field region confirm that the two type 3 coppers are oxidized and antiferromagnetically coupled and that the type 2 copper is reduced. In addition, the charge transfer (CT) absorption spectrum of the intermediate supports a μ-1, 1 hydroperoxide description based on a comparison to Cu(II)−peroxo model spectra. The decay of the T1Hg Lc oxygen intermediate is pH dependent, slow, and proceeds through an additional intermediate with an MCD spectrum in the CT region analogous to that of the oxygen intermediate in the native enzyme which is at least one electron further reduced. These studies lead to a spectroscopically effective model for peroxide bound to the trinuclear copper cluster site in the intermediate, and provide significant insight into the molecular mechanism of the catalytic reduction of dioxygen to water by the multicopper oxidases.

Introduction

Laccase (Lc), ascorbate oxidase, and ceruloplasmin are the known multicopper oxidases which catalyze the 4-electron reduction of dioxygen to water.[1−4] Laccase (*p*-diphenol: dioxygen oxidoreductase, EC 1.10.3.2) is the simplest of the multicopper oxidases containing a total of four copper centers which are divided into three types: type 1, a blue copper center with characteristic spectral features (an intense absorption band at ∼600 nm (ϵ ∼5000 M^{-1} cm^{-1}) and a small parallel hyperfine coupling ($A_{\|}$ ∼ 40−70 × 10^{-4} cm^{-1}) in the EPR spectrum); type 2, a mononuclear copper center with normal spectral features; and type 3, a binuclear copper site where the coppers are antiferromagnetically coupled through a bridging ligand, hence EPR silent.[5,6] Ascorbate oxidase[7−9] can be described as a dimer of laccase sites with a total of eight coppers, while ceruloplasmin[10,11] contains at least two type 1, one type 2, and one type 3 center. Antiferromagnetically coupled sites are also present in the binuclear copper proteins hemocyanin and tyrosinase,[3,12] which reversibly bind and activate dioxygen, respectively.

Spectroscopy combined with crystallography have generated a detailed description of the active site in laccase and ascorbate oxidase. Magnetic circular dichroism (MCD)[6,13,14] and X-ray absorption spectroscopy[15] on laccase have shown that the type 2 and type 3 centers combine to function as a trinuclear copper cluster with respect to exogenous ligand interactions including the reaction with dioxygen. Crystallography[8,9] also shows the

* To whom all correspondence should be addressed.
[†] Department of Chemistry, Stanford University.
[‡] Stanford Synchrotron Radiation Laboratory.
[⊗] Abstract published in *Advance ACS Abstracts,* March 15, 1996.

(1) Malkin, R.; Malmström, B. G. *Adv. Enzymol. Relat. Areas Mol. Biol.* **1970**, *33*, 177.
(2) Malmström, B. G.; Andréasson, L.-E.; Reinhammar, B. In *Enzymes*, 3rd ed.; Boyer, P. D., Ed.; Academic: New York, NY, 1975; Vol. 12, p 507.
(3) Solomon, E. I.; Baldwin, M. J.; Lowery, M. D. *Chem. Rev.* **1992**, *92*, 521.
(4) Solomon, E. I.; Lowery, M. D. *Science* **1993**, *259*, 1575.
(5) Dooley, D. M.; Scott, R. A.; Ellinghaus, J.; Solomon, E. I.; Gray, H. B. *Proc. Natl. Acad. Sci. U.S.A.* **1978**, *75*, 3019.
(6) Cole, J. L.; Clark, P. A.; Solomon, E. I. *J. Am. Chem. Soc.* **1990**, *112*, 9534.
(7) Mondoví, B.; Avigliano, L. In *Copper Proteins and Copper Enzymes*; Lontie, R., Ed.; CRC Press, Inc.: Boca Raton, FL, 1984; Vol. III, p 101.
(8) Messerschmidt, A.; Rossi, A.; Ladenstein, R.; Huber, R.; Bolognesi, M.; Guiseppina, G.; Marchesini, A.; Petruzzelli, R.; Finazzi-Agro, A. *J. Mol. Biol.* **1989**, *206*, 513.
(9) Messerschmidt, A.; Ladenstein, R.; Huber, R.; Bolognesi, M.; Avigliano, L.; Petruzzelli, R.; Rossi, A.; Finazzi-Agrò, A. *J. Mol. Biol.* **1992**, *224*, 179.
(10) Ryden, L. In *Copper Proteins and Copper Enzymes*; Lontie, R., Ed.; CRC Press: Boca Raton, FL, 1984; Vol. III, p 37.
(11) Calabrese, L.; Carbonaro, M.; Musci, G. *J. Biol. Chem.* **1988**, *263*, 6480.
(12) Magnus, K. A.; Ton-That, H.; Carpenter, J. E. In *Bioinorganic Chemistry of Copper*; Karlin, K. D., Tyeklar, Z., Eds.; Chapman & Hall: New York, 1993; p 143.
(13) Allendorf, M. D.; Spira, D. J.; Solomon, E. I. *Proc. Natl. Acad. Sci. U.S.A.* **1985**, *82*, 3063.
(14) Spira-Solomon, D. J.; Allendorf, M. D.; Solomon, E. I. *J. Am. Chem. Soc.* **1986**, *108*, 5318.
(15) Cole, J. L.; Tan, G. O.; Yang, E. K.; Hodgson, K. O.; Solomon, E. I. *J. Am. Chem. Soc.* **1990**, *112*, 2243.

0002-7863/96/1518-3202$12.00/0

presence of this trinuclear copper cluster in ascorbate oxidase and indicates that the type 2 center is 3-coordinate with two histidines and a water as ligands and the type 3 coppers are 4-coordinate each having three histidine ligands and are bridged by hydroxide. All coppers of the type 2/type 3 trinuclear copper cluster are within 3.8 Å of each other. The type 1 site is approximately 12.5 Å away from the trinuclear cluster but connected to it by a type 1 − Cys − His − type 3 pathway for electron transfer. In the crystal structure of the reduced enzyme,[16] the coordination environments of the type 1 and type 2 centers are unchanged while the hydroxide bridge at the type 3 site is no longer present and the two type 3 coppers are now separated by 5.1 Å. A structure for the peroxide adduct of fully oxidized ascorbate oxidase has also been reported[16] (*vide infra*).

The reaction of fully (i.e., 4 electron) reduced laccase has been studied in some detail and a number of mechanisms have been proposed.[16−18] There is one intermediate observed in the reaction of the reduced native enzyme with dioxygen, which shows an $S = {}^1/_2$ EPR signal at <20 K which broadens with $^{17}O_2$.[19−21] It had been thought to be a three-electron reduced oxygen radical with the electrons contributed by the type 1 and the two type 3 coppers which are oxidized in the native intermediate, while the type 2 was thought to be reduced based on the lack of its EPR signal. However, MCD studies[22] have shown that the $S = {}^1/_2$ center in the native intermediate has significant Cu(II) character leading to an alternative description of the native intermediate as a 4-electron reduced hydroxide product bound to a fully oxidized trinuclear cupric site. No other intermediates (i.e., peroxide-level) are observed at earlier stages of reduction of dioxygen by the native enzyme. Two derivatives of laccase have been useful in defining the metal center requirements for oxygen reduction. The type 2 depleted (T2D) derivative[23] has the type 2 center reversibly removed and thus contains only the type 1 and the type 3 centers. Reduced T2D laccase does not react with dioxygen, demonstrating the requirement of the type 2 center for oxygen reduction. The second derivative, T1Hg Lc,[24,25] has the type 1 center replaced by a redox inactive Hg^{2+} ion but still contains an intact type 2/type 3 trinuclear copper cluster site. The fully (i.e., 3 electron) reduced T1Hg Lc derivative reacts with dioxygen showing that the type 2/type 3 trinuclear copper cluster is the minimum structural unit for dioxygen reduction.[15]

The type 1 center in the T1Hg Lc derivative is no longer capable of transferring an electron to dioxygen reacting at the trinuclear copper site. This has enabled us to generate a new oxygen intermediate[26] which is at least one electron less reduced than the native intermediate described above. The rate of formation of the T1Hg Lc oxygen intermediate is the same as that of the oxygen intermediate of native Lc,[26] indicating that the T1Hg Lc oxygen intermediate can be the precursor to the native oxygen intermediate, and formation of the T1Hg Lc oxygen intermediate is the rate-determining step in the formation of the native Lc intermediate. Our preliminary spectral studies[26] on the T1Hg Lc intermediate indicated that two electrons had been transferred to dioxygen and thus this is a peroxide level intermediate. In the present study we have investigated the properties of this intermediate in detail using a wide variety of spectral techniques. We have developed a structural model for the intermediate bound to the trinuclear cluster and obtained significant insights into the catalytic mechanism of the four-electron reduction of dioxygen to water.

Experimental Section

Rhus vernicifera laccase was isolated[27,28] from the acetone powder (Saito and Co., Osaka, Japan). Laccase activity was assayed spectrophotometrically using *N*,*N*-dimethyl-*p*-phenylenediamine as a substrate.[27] The T1Hg derivative of laccase was prepared using a hollow fiber dialysis unit (Spectrum Medical Instruments, Los Angeles) according to published procedures.[24,25,29] The concentration of T1Hg Lc was measured using the absorption band at 280 nm, the extinction coefficient of which was either taken to be 90 000 M^{-1} cm^{-1} [30] or was calculated on the basis of the A_{280}/A_{614} ratio of native laccase (ϵ_{614} = 5700 M^{-1} cm^{-1}).[6] Copper concentration was determined spectrophotometrically by the method of Felsenfeld using 2,2′-biquinoline[31] or by atomic absorption spectroscopy. All experiments were performed in 100 mM potassium phosphate buffer, pH = 7.4 at room temperature unless otherwise specified.

For all experiments except isotope ratio mass spectrometry T1Hg Lc was reduced by anaerobic dialysis against 5 mM sodium dithionite in 100 mM potassium phosphate buffer at pH = 7.4 followed by anaerobic dialysis three times against the same buffer without dithionite. The final dialysis step was performed against 100 mM potassium phosphate in D_2O (99.9 atom % D, Aldrich), pD = 7.0, for SQUID magnetic susceptibility and against 40% (v/v) glycerol−100 mM potassium phosphate buffer for EXAFS. For isotope ratio mass spectrometry (IRMS), T1Hg Lc was reduced by directly adding three electron equivalents of dithionite to the deoxygenated protein solution under strictly anaerobic conditions. The concentration of dithionite was measured using the absorption at 316 nm (ϵ_{316} = 8000 M^{-1} cm^{-1}).[32] The oxygen intermediate was prepared by mixing equal volumes of reduced protein and oxygen saturated buffer for absorption and CD. For IRMS, reduced protein was mixed with $^{18}O_2$ (Isotec 99% or Cambridge Isotope 97−99%), for SQUID susceptibility, EPR, Cu K edge, and EXAFS, the reduced protein was oxygenated by stirring in air, and for MCD samples, reduced protein was mixed with oxygen-saturated glycerol. Glycerol was required to make good-quality low-temperature glasses for MCD and EXAFS studies. The edge samples were prepared without the addition of glycerol since glasses were not required to obtain high-quality edge data. Note that the two methods of preparing reduced samples give different rates of decay of the intermediate ($t_{1/2}$(excess dithionite followed by dialysis) ∼ 55 min and $t_{1/2}$(stoichiometric) = 9.8 min, *vide infra*). However, the intermediates obtained from the two methods of reduction exhibit the same spectral features. Further, preparing an intermediate sample from T1Hg Lc obtained in reduced form directly from the preparation gives the same spectral features as the intermediates obtained by the above dithionite reduction procedures. The rate of its decay is comparable to that obtained by stoichiometric reduction. All chemicals were reagent grade and were used without further purification. Water was purified to a resistivity of 15−18 MΩ cm using a Barnstead Nanopure deionizing system.

(16) Messerschmidt, A.; Luecke, H.; Huber, R. *J. Mol. Biol.* **1993**, *230*, 997.
(17) Reinhammar, B. In *Copper Proteins and Copper Enzymes*; Lontie, R., Ed.; CRC Press: Boca Raton, FL, 1984; Vol. III, p 1.
(18) Farver, O. In *Gas Enzymology, Proceedings of a Symposium, 1984*; Degn, H., Cox, R. P., Toftlund, H., Eds.; Reidel: Dordrecht, The Netherlands, 1985; p 61.
(19) Deinum, J.; Vänngård, T. *FEBS Lett.* **1975**, *58*, 62.
(20) Aasa, R.; Brändén, R.; Deinum, J.; Malmström, B. G.; Reinhammar, B.; Vänngård, T. *Biochem. Biophys. Res. Commun.* **1976**, *70*, 1204.
(21) Brändén, R.; Deinum, J. *FEBS Lett.* **1977**, *73*, 144.
(22) Clark, P. A.; Solomon, E. I. *J. Am. Chem. Soc.* **1992**, *114*, 1108.
(23) Graziani, M. T.; Morpurgo, L.; Rotilio, G.; Mondoví, B. *FEBS Lett.* **1976**, *70*, 87.
(24) Morie-Bebel, M. M.; Morris, M. C.; Menzie, J. L.; McMillin, D. R. *J. Am. Chem. Soc.* **1984**, *106*, 3677.
(25) Severns, J. C.; McMillin, D. R. *Biochemistry* **1990**, *29*, 8592.
(26) Cole, J. L.; Ballou, D. P.; Solomon, E. I. *J. Am. Chem. Soc.* **1991**, *113*, 8544.
(27) Reinhammar, B. *Biochim. Biophys. Acta* **1970**, *205*, 35.
(28) Reinhammar, B. *Biochim. Biophys. Acta* **1972**, *275*, 245.
(29) Morie-Bebel, M. M.; Menzie, J. L.; McMillin, D. R. In *Biological & Inorganic Copper Chemistry, Proceedings of the Conference on Copper Coordination Chemistry, 2nd, 1984*; Karlin, K. D., Zubieta, J., Eds.; Adenine Press: Guilderland, NY, 1986; Vol. 1, p 89.
(30) Meadows, K. A.; Morie-Bebel, M. M.; McMillin, D. R. *J. Inorg. Biochem.* **1991**, *41*, 253.
(31) Felsenfeld, G. *Arch. Biochem. Biophys.* **1960**, *87*, 247.
(32) Dixon, M. *Biochim. Biophys. Acta* **1971**, *226*, 241.

UV/visible absorption spectra were recorded on a Hewlett-Packard HP8452A diode array spectrophotometer in either 1-cm, 2-mm, or 1-mm quartz cuvettes. CD spectra were recorded using 1-cm or 2-mm quartz cuvettes. MCD data were obtained using a sample cell consisting of two quartz disks with a 3-mm rubber spacer. CD and MCD spectroscopy were performed with a Jasco J-500-C spectropolarimeter operating with S-1 and S-20 photomultiplier tubes for the 1050−800- and 800−300-nm regions, respectively. For MCD spectroscopy low temperatures were achieved using an Oxford Spectromag 4 superconducting magnet/cryostat as previously described.[6] The frozen intermediate was prepared in the sample holder and directly loaded into the chamber of the MCD magnet. The possibility of strain-induced depolarization of light by the sample glass was evaluated by a comparison of the CD spectra of a solution of nickel tartrate placed before and after the sample; depolarizations of <10% were routinely obtained. Sample temperatures were measured with a carbon glass resistor (Cyrogenic Calibrations, Pitchcott, Aylesbury, Buckinghamshire, U.K.). Spectra were generally recorded at 4.2 K and 5 T. MCD intensity is reported in units of M^{-1} cm^{-1} T^{-1}.

Measurements of the $H_2{}^{18}O/H_2{}^{16}O$ isotope ratio in the solvent were made using a Finnigan 251 isotope ratio mass spectrometer equipped with automated sample injection and having a built-in automated CO_2-H_2O equilibration device based on the method developed by Epstein and Mayeda.[33] Reduced T1Hg Lc (1.0 mL, 0.33 mM) was reacted with $^{18}O_2$. A water sample (about 200 μL) was collected between 1 and 6 min after mixing for IRMS experiments using a centricon concentration device (50 000 MW cutoff, Amicon Inc.) by centrifuging at 5800 g using an RC-5 Sorvall centrifuge. A 400 μL aliquot from the protein remaining in the centricon vial after water collection was transferred to an EPR tube and frozen quickly in a hexane−LN_2 bath. The spin quantitation of the 77 K EPR spectrum of this sample was used to evaluate the amount of intermediate that had decayed during the time of water collection. The collected water sample was equilibrated with CO_2 gas for 2 days and the isotope ratio of $C^{18}O^{16}O/C^{16}O^{16}O$ (mass 46 vs 44) was measured by injecting 200 μmol of the equilibrated gas. This measured ratio is equal to the ratio of $H_2{}^{18}O/H_2{}^{16}O$ in the water sample at equilibrium.[33]

EPR spectra were obtained with a Bruker ER 220-D-SRC spectrometer. Sample temperatures of 77 K were maintained using a liquid N_2 finger dewar, and temperatures from 70 to 4 K were obtained using an Air Products Model LTR Helitran liquid helium transfer refrigerator and a Lake Shore Cryotronics temperature controller Model DTC-500. The EPR data were spin quantitated against a Cu standard (1.0 mM $CuSO_4 \cdot 5H_2O$ with 2 mM HCl and 2 M $NaClO_4$[34]). Spectra Calc, Collect Arithmetic C2.20 from Galactic Industries Corp. was used for spin integration of the EPR signals.

Magnetic susceptibility data were collected on a Quantum Design Model MPMS SQUID magnetometer. Mercury tetrathiocyanatocobaltate(II) and a palladium cylinder were employed as dual magnetometer calibrants. Polycarbonate capsules (Universal Plastics and Engineering Co., Rockville, MD) were used as sample buckets. The two halves of the capsule were sealed by applying a drop of acetone and the cap had a hole to allow the space above the sample to be evacuated in the antechamber, prior to sample loading. The antechamber was flushed with He gas prior to sample loading. Samples were loaded frozen onto a phenolic guide (clear soda straw) which was fixed to the end of a magnetometer drive rod and loaded into the SQUID magnetometer. After susceptibility measurements on the intermediate were complete, the sample was thawed and allowed to decay at 4 °C for 2 days. This decayed fully oxidized sample served as the reference for the intermediate data. Sample volumes were typically 100 μL and the concentration was ~1.3 mM in T1Hg Lc. The susceptibility versus $1/T$ data were taken in the 10−50 K region at 4.0 T and fit using a linear least-squares procedure. Saturation data were taken at 2 K.

X-ray absorption spectroscopic data for the reduced, oxidized, and oxygen intermediate of T1Hg Lc were recorded at the Stanford Synchrotron Radiation Laboratory (SSRL) on unfocused beamline 7-3 under dedicated conditions (3.0 GeV, 60−100 mA). Monochromatic radiation was obtained using a Si(220) double-crystal monochromator which was detuned 50% for harmonic rejection. The fluorescence signals were measured with an ionization chamber detector[35,36] equipped with Soller slits and a Ni filter. Internal energy calibration was performed assigning the first inflection point of the Cu foil spectrum to be 8980.3 eV. The samples were loaded into 2 mm thick Lucite XAS cells with 63.5 μm Mylar windows, immediately frozen, and kept under LN_2 prior to the measurements. The samples were maintained at a constant temperature of 10 K by an Oxford Instruments CF1208 continuous-flow liquid-helium cryostat during the measurements. The Cu concentrations for the intermediate, reduced, and decayed fully oxidized T1Hg Lc were 3.6, 6.0, and 3.6 mM, respectively, for the edge samples and 4.2, 6.0, and 9.0 mM, respectively, for the EXAFS samples.

The T1Hg Lc intermediate samples used for these XAS measurements contained 34% fully oxidized sample due to decay of the intermediate. Both the oxidized and the intermediate T1Hg Lc samples were monitored for photoreduction throughout the course of data collection. A gradual increase in the intensity of the pre-edge feature at 8984 eV is indicative of photoreduction from Cu(II) to Cu(I). The two edge samples showed no evidence of photoreduction during a total of 5 scans measured for each sample and therefore the average of the 5 scans was used for the edge analysis. For the two EXAFS samples, a trend of photoreduction was observed and so only the scans with less than 5% photoreduction (14 scans for intermediate and 5 scans for the fully oxidized sample) compared with the first scan were averaged. The scans were collected out to $k = 9$ Å^{-1} for edge data and $k = 13.4$ Å^{-1} (up to the zinc K edge) for EXAFS data. It was found that zinc was present in low concentration in all the samples. All the data were processed using standard procedures for pre-edge subtraction, spline fit and removal, and normalization.[37−39]

The edge region of the intermediate sample was analyzed by comparison with simulated edges calculated using data from a 4-coordinate Cu(II) model and a 2-, 3-, or 4-coordinate Cu(I) model with appropriate weighting, taking into account the amount of Cu(II) produced upon decay of the intermediate. The model compounds used for the simulated edge are the fully oxidized T1Hg Lc for Cu(II), $[(Mepy_2)Cu(CH_3CN)ClO_4]$[40] for 4-coordinate Cu(I), reduced T1Hg Lc for 3-coordinate Cu(I), and $[Cu(1,2MeIm)_2](PF_6)$[40] for 2-coordinate Cu(I).

The empirical EXAFS data analyses were performed with non-linear least-squares curve-fitting techniques.[37−39] The following models were used to obtain the empirical phase and amplitude parameters: Cu−O from Cu(acetylacetonate)$_2$[41], Cu−N from Cu(imidazole)$_4(NO_3)_2$,[42] and Cu−Cu from $[Cu(HB(3,5\text{-}i\text{-}Pr_2pz)_3)]_2(OH)_2$.[43] Fourier transforms were calculated over the data range of 3.5−12.5 Å^{-1} with a Gaussian window of 0.1 Å^{-1} and were then backtransformed with a Fourier filtering window centered on the peak of interest (see Results and Analysis section). All curve fitting was performed with k^3-weighted data by varying the structure-dependent parameters, either the distance and Debye−Waller (DW) factor with fixed coordination number (CN) or distance and variable CN with fixed DW factor.

Results and Analysis

(A) Decay Kinetics. Figure 1A presents the time course of the decay of the intermediate of T1Hg Lc at pH = 7.4 at room temperature as monitored by optical absorption spectroscopy in the 300−820-nm region. The first spectrum (light solid line)

(33) Epstein, S.; Mayeda, T. *Geochim. Cosmochim. Acta* **1953**, *4*, 213.
(34) Carithers, R. P.; Palmer, G. *J. Biol. Chem.* **1981**, *256*, 7967.
(35) Stern, E. A.; Heald, S. M. *Rev. Sci. Instrum.* **1979**, *50*, 1579.
(36) Lytle, F. W.; Greegor, R. B.; Sandstrom, E. R.; Marques, E. C.; Wong, J.; Spiro, C. L.; Huffman, G. P.; Huggins, R. E. *Nucl. Instrum. Methods* **1984**, *226*, 542.
(37) Scott, R. A. *Methods Enzymol.* **1985**, *117*, 414.
(38) Cramer, S. P.; Hodgson, K. O.; Stiefel, E. I.; Newton, W. E. *J. Am. Chem. Soc.* **1978**, *100*, 2748.
(39) Cramer, S. P.; Hodgson, K. O. *Prog. Inorg. Chem.* **1979**, *15*, 1.
(40) The compounds were kindly provided by Prof. K. D. Karlin's laboratory at Johns Hopkins University.
(41) Starikova, Z. A.; Shugam, E. A. *Zh. Struckt. Khim.* **1969**, *10*, 290.
(42) McFadden, D. L.; McPhail, A. T.; Garner, C. D.; Mabbs, F. E. *J. Chem. Soc., Dalton Trans.* **1976**, 47.
(43) Kitajima, N.; Fujisawa, K.; Fujimoto, C.; Moro-oka, Y.; Hashimoto, S.; Kitagawa, T.; Toriumi, K.; Tatsumi, K.; Nakamura, A. *J. Am. Chem. Soc.* **1992**, *114*, 1277.

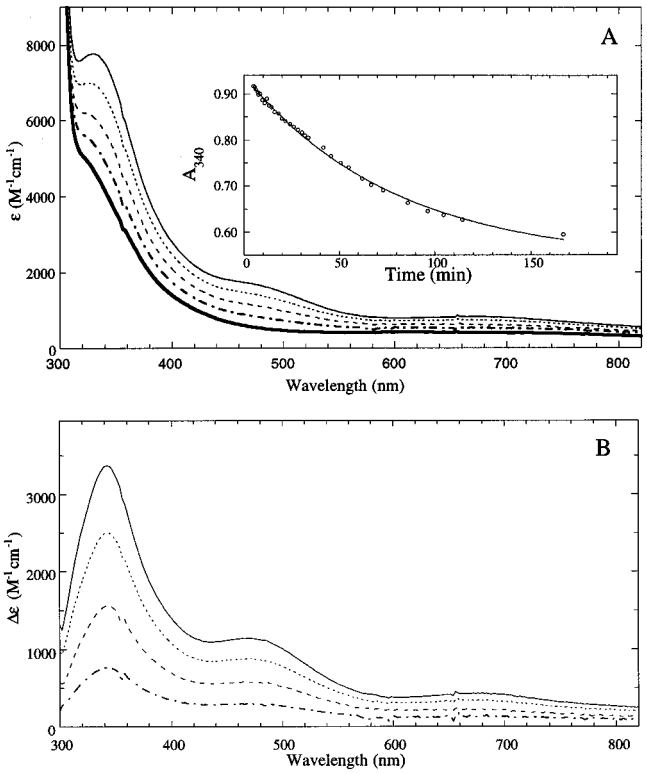

Figure 1. (A) Absorption spectra of the intermediate at various times during its decay: (—) 6 min, (•••) 33 min, (- - -) 73 min, (—•—) 170 min, (dark solid line) fully oxidized at room temperature, pH = 7.4. The inset shows the kinetics of decay of the intermediate, monitored by the amplitude of the 340-nm band: The data were fit to a single exponential with a first-order rate constant of 0.013(±0.001) min^{-1}. (B) Absorption difference spectra of each intermediate spectrum in (A) relative to that of fully oxidized T1Hg Lc.

is that of the intermediate recorded 6 min after reaction of the reduced protein with dioxygen and the last (dark solid line) is that of the fully oxidized protein. The difference spectra of the intermediate sample prepared at different time points during the decay, after subtraction of the fully oxidized protein, are shown in Figure 1B. The difference spectra clearly exhibit bands at 340 and 470 nm which decrease in intensity as the intermediate decays, indicating that these bands are associated with the intermediate (see CT Absorption/CD section E(2)). The inset in Figure 1A shows the absorbance at 340 nm plotted as a function of time. The data points can be fit with a single exponential curve with a first-order rate constant of 0.013-(±0.001) min^{-1} ($t_{1/2}$ = 53 (±4) min). The type 2 Cu EPR signal is found to increase in intensity as the intermediate decays (Figure 2). The kinetics of the appearance of the type 2 EPR signal (k = 0.011(±0.001) min^{-1}, $t_{1/2}$ = 63(±6) min) parallels that of the disappearance of the absorption bands in the intermediate (Figure 2, inset). The pH dependence of the decay of the intermediate was monitored between pH = 4.0 and 7.4 at room temperature using the 340-nm absorption band, and the data in each case were fit with a single exponential curve. The rate constants thus obtained are plotted as a function of pH in Figure 3, which shows that rate of decay of the intermediate increases as the pH is lowered. Thus high pH conditions were used to stabilize the intermediate for spectral studies and the intensity of the EPR signal of type 2 has been used throughout the study to estimate the extent of decay of the intermediate to fully oxidized T1Hg Lc.

The dependence on pH implies proton involvement in the decay. If a proton is required in the rate law for the decay process, i.e. the protonation step is slow (eq 1, where E_{int} is the

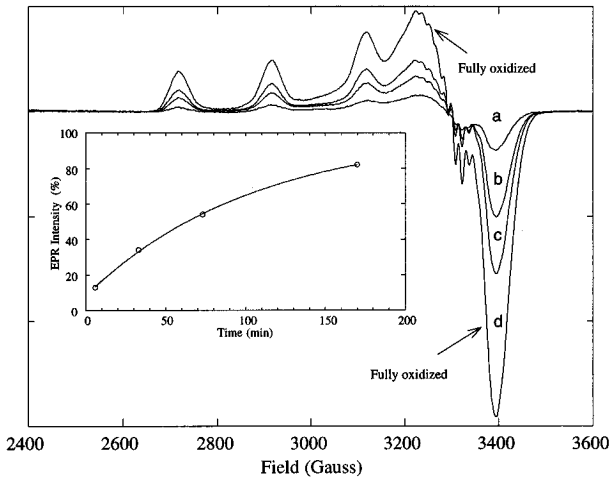

Figure 2. EPR spectra of the intermediate at various times during its decay: (a) 6 min, (b) 33 min, (c) 73 min, (d) fully oxidized at room temperature and pH = 7.4. Inset shows the kinetics of increase of EPR intensity. The data were fit to a single exponential with a first-order rate constant of 0.011(±0.001) min^{-1} for the decay of the intermediate.

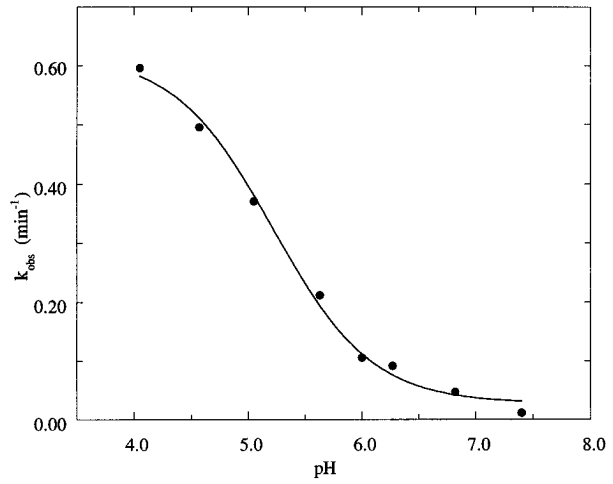

Figure 3. Decay rate of the intermediate as a function of pH. Aliquots of the reduced protein in 10 mM phosphate, pH = 7.4, were injected into 100 mM phosphate or acetate buffers pre-equilibrated with oxygen which were adjusted to different pHs. The actual pH of the solution was determined after the decay using a glass electrode. The solid line is the best fit to the protonation equilibrium model, Scheme 1 in the text.

intermediate, E_{ox} is reoxidized T1Hg Lc, x is the number of protons needed per mole of intermediate),

$$E_{int} + xH^+ \xrightarrow{k_1} E_{ox} \quad (1)$$

then, the observed rate of the reaction, k_{obs}, is given by eq 2.

$$k_{obs} = k_1[E_{int}][H^+]^x \quad (2)$$

Equation 2 predicts a linear relationship between log k_{obs} and pH which is not observed. Therefore, the protonation step is not the rate-determining step in the decay of the intermediate.

Alternatively, a protonation equilibrium step for the intermediate does explain the pH dependency of the decay (Scheme 1, where, k_2 and k_2' are rate constants for the decay of unprotonated and protonated forms of the intermediate and $K_{a,int}$ and $K_{a,ox}$ are acid dissociation constants for the intermediate and the oxidized enzyme). Since the formation of the intermediate is much faster than its decay ($k = 5 \times 10^6$ M^{-1} s^{-1} for

Scheme 1

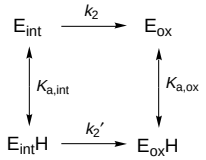

formation at room temperature[26]), the rate of formation does not affect the observed rate constant. The observed rate constant for decay of the intermediate in Scheme 1 is given in eq 3.[44]

$$k_{obs} = \frac{k_2'[H^+] + k_2 - K_{a,int}}{K_{a,int} + [H^+]} \quad (3)$$

The pH dependence data in Figure 3 were fit to eq 3 with the solid line showing the best fit to the data. The following parameters were obtained: $k_2' = 0.62(\pm0.04)$ min^{-1}, $k_2 = 6.1(\pm1.0) \times 10^{-6}$ min^{-1}, and $K_{a,int} = 6.0(\pm1.0) \times 10^{-6}$ M, p$K_{a,int} = 5.2(\pm0.1)$. Since k_2' is 10^6-fold higher than k_2, the predominant decay pathway is through k_2'. This indicates that the intermediate is protonated prior to its decay. Protonation may occur at an amino acid residue is the vicinity of the active site or directly at the oxygen intermediate bound to the protein. If protonation occurs directly at the oxygen intermediate, the charge transfer spectra of the protonated and unprotonated intermediate should be significantly different. Since the rate of decay of the protonated intermediate is still relatively slow ($k_{obs} = 0.60(\pm0.06)$ min^{-1} at pH = 4.0), this difference should be observable. Our absorption data do not show a significant change in intensity at 340 nm in intermediate samples prepared from pH = 4.0 to 7.4. This observation combined with the pK_a of 5.2 suggests that a nearby residue might be involved in the protonation.

(B) Isotope Ratio Mass Spectrometry (IRMS). Isotope ratio mass spectrometry is designed to measure small changes in isotope ratio and has been applied to native laccase.[45] Water samples were collected by vacuum distillation after reacting reduced laccase with $^{18}O_2$ and the increase in $H_2{}^{18}O$ content in these samples was determined by IRMS. This experiment showed that one $H_2{}^{18}O$/molecule of laccase is released into the solution just after turnover while the second oxygen remains bound to the protein and slowly exchanges with the solvent water over 24 h.[45] We have applied this technique to determine the number of water molecules that stay bound in the oxygen intermediate of T1Hg Lc by measuring the amount of $H_2{}^{18}O$ released after reacting reduced T1Hg Lc with $^{18}O_2$. The procedure for water collection has been modified to use a centricon concentration device, which uses centrifugal force to extract water from the protein solution, instead of vacuum distillation which introduces errors due to isotopic fractionation.[46] Reduced T1Hg Lc was prepared by adding three electron equivalents of sodium dithionite to the deoxygenated protein solution under anaerobic conditions. This reduced protein was then reacted with $^{18}O_2$ and the water sample was collected from the reacted protein solution after various times. The collected water sample was equilibrated with CO_2 gas for 2 days and the isotope ratio of $C^{18}O^{16}O/C^{16}O^{16}O$ (mass 46 vs 44) was measured by injecting 200 μmol of the equilibrated gas into the mass spectrometer. This measured ratio is equal to the ratio of $H_2{}^{18}O/H_2{}^{16}O$ in the water sample at equilibrium.[33]

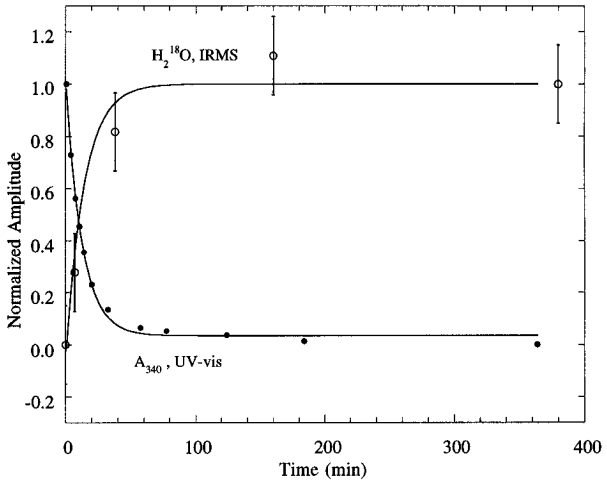

Figure 4. Kinetics of release of $H_2{}^{18}O$ measured by isotope ratio mass spectrometry: (○) amount of H_2O^{18} released; (●) decay of intermediate from optical absorption at 340 nm. Conditions: 0.33 mM of T1Hg laccase concentration, room temperature. Reduced protein was prepared by adding 3 electron equivalents of dithionite. The solid lines are single exponential fits to the data. Rate constants are 0.081(±0.01) min^{-1} ($t_{1/2} = 8.6(\pm1)$ min) for the 340-nm absorption band and 0.071(±0.007) min^{-1} ($t_{1/2} = 9.8(\pm1)$ min) for the $H_2{}^{18}O$ release.

Table 1. Increase of $H_2{}^{18}O$ in Water Samples after Reaction of Reduced T1Hg Lc with $^{18}O_2$ at 4 °C

sample	enzyme[a] (mM)	$H_2{}^{18}O$/molecule of T1Hg Lc[b]
1	0.29	0.47 (±0.13)
2	0.30	0.41 (±0.14)
3	0.31	0.45 (±0.13)
		av 0.44 (±0.23)

[a] The concentration of reduced T1Hg Lc was determined by subtraction of the amount of oxidized form present in the reduced protein (reduction done using 3-electron equivalents of dithionite) from the initial protein concentration. The amount of oxidized form present in the reduced sample was determined by the type 2 LN_2 EPR intensity which varied between 10 and 13% depending on preparation. [b] The intermediate decayed 19% (±6%) during the time of water collection (1−6 min after reaction).

The increase in $H_2{}^{18}O$ content in the solution was measured relative to a control sample where water was collected from reduced protein without reaction with $^{18}O_2$. In these experiments we could determine a change in $H_2{}^{18}O$ content with 0.03 mM precision.

Water samples were prepared at a series of times during the intermediate decay at room temperature and the increase of $H_2{}^{18}O$ in each sample was measured (Figure 4). The release of $H_2{}^{18}O$ followed the same kinetics as the decay of the intermediate by optical absorption and EPR spectroscopies ($t_{1/2} = 9.8(\pm1)$ min under stoichiometric reduction conditions). Water samples were then collected between 1.0 and 6.0 min after the reaction of reduced T1Hg Lc with $^{18}O_2$ at 4 °C, where the lower temperature was used to slow the decay rate which helped in sample collection during early stages of decay. This was done to determine the number of water molecules released during the formation of the intermediate. The experimentally determined increase in $H_2{}^{18}O$ content in the water samples was 0.44(±0.23) per protein molecule from three independent experiments as given in Table 1. The average decay of the intermediate during the time period of water collection was estimated by the LN_2 EPR intensities of the protein samples before and after water collection. This was determined to be 19(±6)% for the three sets of samples. The amount of $H_2{}^{18}O$ detected by IRMS would be the sum of the amount of water released during formation of the intermediate and that released

(44) Fersht, A. *Enzyme Structure and Mechanism*, 2nd ed.; W. H. Freeman and Company: New York, 1985.
(45) Brändén, R.; Deinum, J.; Coleman, M. *FEBS Lett*. **1978**, *89*, 180.
(46) Stable Isotope Hydrology-Deuterium and Oxygen-18 in the water cycle. International Atomic Energy Agency, 210, 1981.

during the 19% decay. If no $H_2{}^{18}O$ was released during the formation of the intermediate, the amount detected should be 0.19 or 0.38 per protein molecule depending on whether one or two $H_2{}^{18}O$ molecules is released upon decay. If one $H_2{}^{18}O$ is released during the formation and one during decay, 1.19 $H_2{}^{18}O$ per molecule of T1Hg Lc should be detected. The experimentally obtained increase of 0.44(±0.23) $H_2{}^{18}O$ per protein molecule is clearly inconsistent with the latter possibility. The results from IRMS thus clearly demonstrate that no water is released during the formation of the intermediate which means that both oxygen atoms are still bound. This indicates its assignment as either a superoxide or peroxide-level intermediate. Only the latter possibility is consistent with X-ray edge data and CD and MCD data in the ligand field region, which show that at least 2 electrons are transferred to O_2 (*vide infra*).

(C) EPR and SQUID Magnetic Susceptibility. X-band EPR studies were performed at liquid nitrogen and liquid helium temperatures to define the ground state spectral properties of the oxygen intermediate of T1Hg Lc. No EPR signals are observed for the intermediate at 77 K except that associated with the type 2 EPR copper due to the 20−30% decay of the intermediate to fully oxidized T1Hg Lc (see Figure 2). Also, EPR data taken at 4 K with microwave powers of up to 200 mW showed no features below $g = 2.0$. This is where the broad signal of the native intermediate[20,47] or the triplet signal of the azide-bound form of T1Hg Lc[6] are observed. Only a partially saturated type 2 EPR signal due to the 20−30% decay of the intermediate to fully oxidized T1Hg Lc is observed. Thus, to determine whether there exists any paramagnetism for the intermediate unobserved by EPR, SQUID magnetic susceptibility measurements were performed.

SQUID susceptibility samples along with corresponding EPR samples were prepared at various times during the course of the intermediate decay to measure the change in paramagnetism. Three sets of experiments gave similar trends. These are shown as saturation magnetization curves in Figure 5A, and clearly demonstrate that the difference in paramagnetism (oxidized − intermediate) decreases with increasing time of intermediate decay. This difference follows the same decay kinetics as the appearance of the type 2 EPR signal, indicating that the change in paramagnetism observed by SQUID magnetic susceptibility parallels the decay of the intermediate. In order to quantitate the amount of paramagnetism in the intermediate by SQUID magnetic susceptibility, the saturation data at 2 K and the susceptibility vs $1/T$ between 11 and 50 K at 4 T were obtained and are given in Figure 5B and the inset, respectively. The final reoxidized sample obtained from the intermediate sample was used as a reference since the difference removes errors caused by the magnetic contribution from the protein, sample holder, dissolved oxygen, etc. Note that the signs of the difference are positive which correspond to excess paramagnetism being present in the oxidized T1Hg Lc relative to the intermediate. This indicates that the intermediate is less paramagnetic than the fully oxidized T1Hg Lc reference sample which has one $S = {}^1/_2$ type 2 site.[6]

The data in Figure 5B and the inset were fit to eqs 4 and 5, respectively,

$$M = Ng\beta S \tanh\left(\frac{g\beta H}{2kT}\right) \tag{4}$$

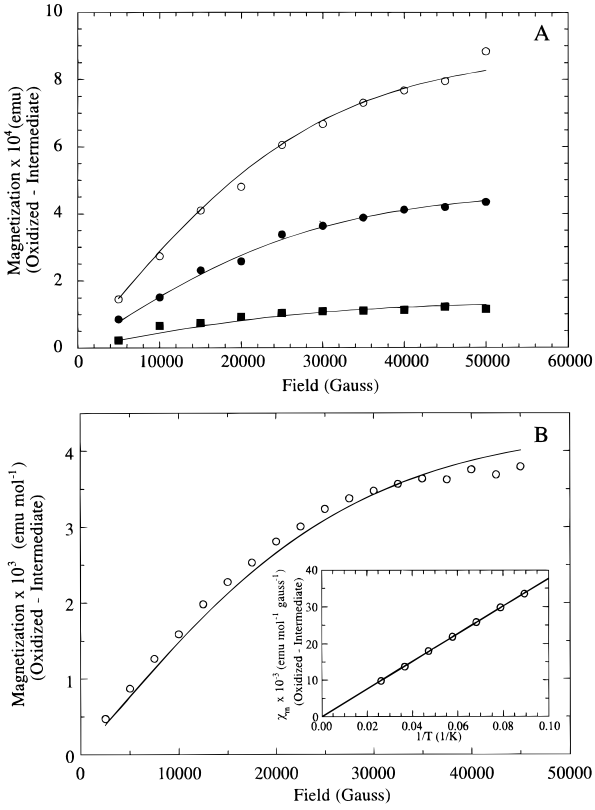

Figure 5. (A) Change of magnetization (fully oxidized − intermediate) during the time course of the decay of the T1Hg Lc intermediate at room temperature: The SQUID magnetization data were collected at a temperature of 2 K. The protein concentration is 1.33 mM. EPR samples were prepared simultaneously to estimate the amount of the decay: (○) 30(±3)%, (●) 52(±5)% (■) 83(±8)%. (B) SQUID magnetic susceptibility (fully oxidized − intermediate) of T1Hg Lc: Protein concentration is 1.36 mM. The intermediate sample contains 36(±4)% fully oxidized T1Hg Lc as determined by EPR. Plot of magnetization data collected at 2 K. The solid line is the best fit to eq 4. Inset: Molar susceptibility between 10 and 50 K at 4 T. χ_m is expressed as susceptibility per mole of T1Hg Lc. The solid line is the best fit to eq 5.

$$\chi_M = \frac{Ng^2\beta^2S(S+1)}{3kT} \tag{5}$$

where M is the magnetization (emu·mol^{-1}), N is Avogadro's number, β is Bohr magneton, k is Boltzmann constant, T is temperature in Kelvin, and χ_m is the molar susceptibility (emu·mol^{-1}·G^{-1}). The g value was set at 2.118 which is an average of g values (2.045, 2.060, 2.250) obtained from the EPR simulation of the resting T1Hg Lc, and the total spin, S, was set at ${}^1/_2$. The difference paramagnetism was quantitated by fitting both the saturation and Curie slope data. The saturation fit gave 0.71(±0.05) and the fit to the Curie slope data gave 0.75(±0.12) spins per molecule. Thus there is an average of 0.73(±0.13) fewer spins per molecule for the intermediate than the fully oxidized T1Hg Lc. Since the fully oxidized T1Hg Lc has one spin per molecule of T1Hg Lc,[6] the paramagnetism of this intermediate sample corresponds to 0.27(±0.13) spins per molecule. The amount of decayed fully oxidized form present in the intermediate sample was estimated to be 36(±7)% by double integration of the EPR signal. The number of spins obtained by SQUID susceptibility and that by EPR agree within error and correspond to the amount of decayed fully oxidized enzyme in the intermediate sample. Thus the pure intermediate has ∼1 less spin ($S = {}^1/_2$) than the fully oxidized T1Hg sample which has a paramagnetic type 2 center.

(47) Aasa, R.; Brändén, R.; Deinum, J.; Malmström, B. G.; Reinhammar, B.; Vänngård, T. *FEBS Lett.* **1976**, *61*, 115.

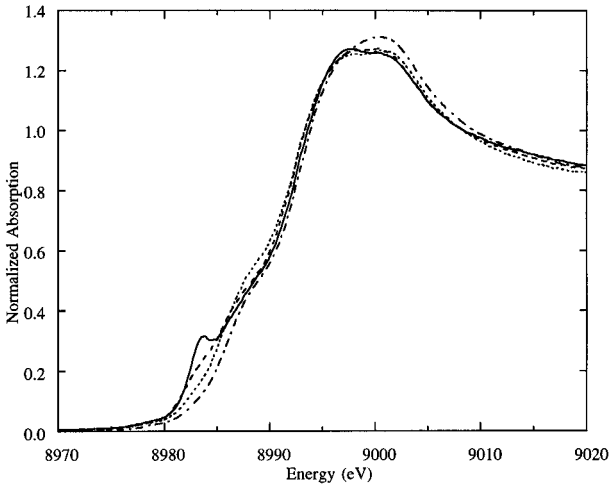

Figure 6. Comparison of the normalized Cu K edge XAS spectrum of the oxygen intermediate of T1Hg laccase (−•−) containing 34(±4)% decayed, fully oxidized T1Hg Lc with simulated edges using 2-(—), 3-(- - -), and 4-(•••) coordinate Cu(I) + 4-coordinate Cu(II) with a ∼1:4 ratio of Cu(I)/Cu(II) (see text).

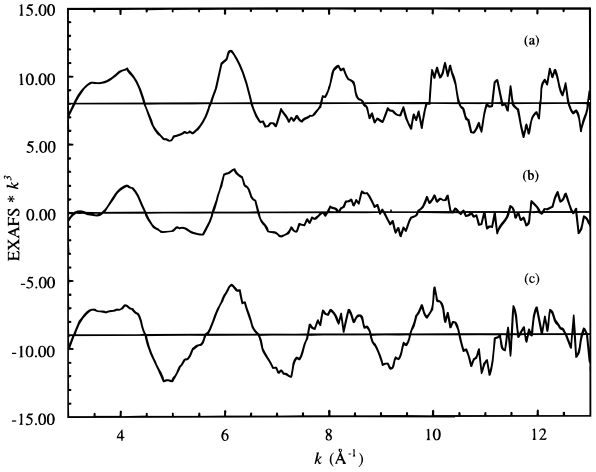

Figure 7. EXAFS spectra of (a) the intermediate, (b) reduced, and (c) oxidized forms of T1Hg laccase. (The ordinate scale is 5 between two consecutive tick marks.)

This requires the oxygen intermediate of T1Hg Lc to be diamagnetic, which combined with XAS and CD and MCD data in the ligand field region (*vide infra*) indicate that the type 2 Cu center is reduced and the type 3 coppers are oxidized and antiferromagnetically coupled. The variable-temperature iso-field data (up to 100 K) of the T1Hg Lc intermediate were fit to the Bleaney−Bowers expression[48] (after subtraction of the paramagnetic contribution due to the type 2 copper resulting from the decay of the intermediate), and a lower limit for the antiferromagnetic coupling of the type 3 centers, $-2J > 200$ cm^{-1}, was obtained from the error limits, indicating that the type 3 coppers are strongly antiferromagnetically coupled.

(D) X-ray Absorption Spectroscopy (XAS). (1) Cu K Edges. The X-ray absorption edges of Cu(I) compounds exhibit a distinctive peak at 8984 eV (assigned as a Cu 1s → 4p transition) which is not found in edges of Cu(II) compounds. This 8984-eV feature has been found to correlate in shape and intensity with the coordination geometry of the cuprous ion.[49] For a linear two-coordinate Cu(I) compound, this feature is rather sharp and intense, whereas for a three-coordinate compound, it appears as a shoulder of significant amplitude on the rising edge. This feature broadens and shifts up in energy for a four-coordinate geometry. Thus the 8984-eV feature is diagnostic of the presence of Cu(I) with a particular coordination geometry.

CD and MCD data in the ligand field region (*vide infra*) and EPR (*vide supra*) indicate that the two type 3 coppers are oxidized and the type 2 copper is reduced in the intermediate of T1Hg Lc. This is strongly supported by the edge spectrum of the intermediate (Figure 6) which shows very little intensity at 8984 eV indicating that most of the coppers present are oxidized. To probe the coordination environment of the reduced type 2 Cu, simulated edges were generated with an appropriately weighted average of Cu(II) and Cu(I) and were compared with the edge of the intermediate sample. The intermediate sample used for XAS contained 34(±4)% fully oxidized T1Hg Lc from decay of the intermediate (from LN_2 EPR), indicating that about one-third of the Cu(I) at the type 2 site had been reoxidized to Cu(II). Therefore, 22(±1)% of the Cu(I) model spectrum was combined with 78(±1)% of the fully oxidized T1Hg Lc spectrum to construct simulated edges, containing 0.66(±0.04) Cu(I) and 2.34(±0.04) Cu(II).

Figure 6 presents the comparison of the Cu K edge of the intermediate sample with the simulated edges having contribution from 2-, 3-, or 4-coordinate Cu(I) models. The component spectra were subjected to energy calibration (within 0.1 eV) and normalization. The simulated edge data using a 2-coordinate Cu(I) model produce a peak of significant intensity at 8984 eV, even with only 22% Cu(I). This 8984-eV pre-edge feature is weaker in the simulated edge using a 3-coordinate Cu(I) model, but is still clearly visible. The edge spectra of the intermediate sample and of the 4-coordinate Cu(I) model, however, do not exhibit a clear 8984-eV feature. The general shape of the edge for the 4-coordinate Cu(I) model follows most closely that of the intermediate sample. These observations are thus consistent with a 4-coordinate type 2 Cu(I) site for the oxygen intermediate of T1Hg Lc.

(2) EXAFS. EXAFS data were obtained for the T1Hg Lc intermediate to gain metrical information on its trinuclear copper center. For comparison, the EXAFS data for the oxidized and the reduced samples were also analyzed. The EXAFS spectra of the three samples are shown in Figure 7 and the Fourier transforms over the k range of 3.5−12.5 Å^{-1} are shown in Figure 8. The data and the results reflect the average of the contributions from all three coppers of the trinuclear center.

First shell curve fits were performed using backtransformed data with a Fourier transform window width as indicated in Table 2. A single O or N wave was first included and the fits were done by stepping through fixed CN while varying the bond distance and the DW factor. As the data reflect the average coordination of three Cu absorbers, and as the sample contained 34% oxidized product, the resulting coordination number would not necessarily be integer. Furthermore, as static disorder, i.e. a spread in distances would be expected, the average coordination number would likely be underestimated, although this would partly be compensated for by a higher DW factor. Both these effects were seen in the fits. The fit for the intermediate T1Hg Lc data gave a minimum at a distance of 1.97 Å for a single Cu−N wave fit and 1.94 Å for a single Cu−O wave fit. The lowest F value (the goodness of fit) occurred for a CN between 3 and 4 (minimum at 3.4). The single-shell fits showed a mismatch in the high k region. Two-shell fits were therefore performed including one N and one O contribution. The minimum was found with 1−2 N/O at 2.03−2.07 Å and 1−2 N/O at ∼1.91 Å (fits 7 and 8 in Table 2). The inclusion of a second wave improved the fits by an average decrease of >25%

(48) Bleaney, B.; Bowers, K. D. *Proc. R. Soc. London* **1952**, *A214*, 451.
(49) Kau, L.-S.; Spira-Solomon, D. J.; Penner-Hahn, J. E.; Hodgson, K. O.; Solomon, E. I. *J. Am. Chem. Soc.* **1987**, *109*, 6433.

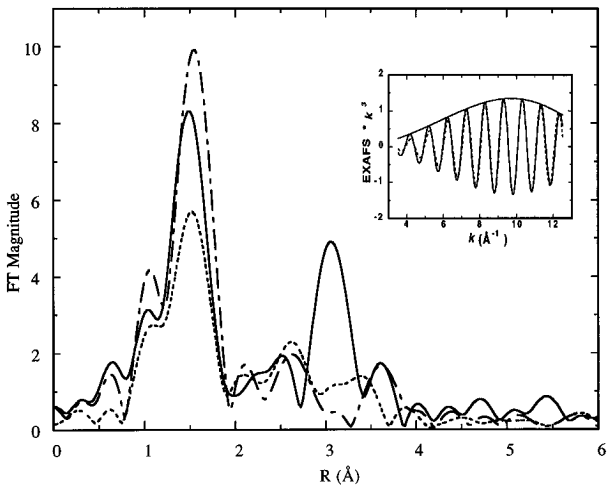

Figure 8. Fourier transforms (FT) of the EXAFS data for the intermediate (dark solid line), reduced (- - -), and oxidized (−·−) forms of T1Hg laccase. The FT peak positions are offset to lower *R* by an atom-dependent phase shift of ∼0.4 Å. Inset: Fourier backtransform of the 3.0-Å peak (*R* window of 2.7 to 3.4 Å) for intermediate T1Hg Lc (—) and the fit to the data (···).

in *F* value. It should be noted that the CNs of Cu−N and Cu−O were highly correlated and so the sum of the two CNs rather than the individual values is a more reasonable overall description. Three-shell fits were also attempted, but the fits gave either an extremely long bond that was chemically unreasonable for the first shell or a collapse of two of the bond distances, indicating that there is no support for a third shell in the data.

The first-shell data for both the oxidized and the reduced T1Hg Lc samples were analyzed using the above approach. The minimum for a single-shell fit for the reduced sample was reached with an average distance of 1.97 (Cu−N) or 1.93 Å (Cu−O). The CNs associated with these fits were between 2 and 3 (minimum at 2.4). Two-shell fits with Cu−N and Cu−O waves did not show significant improvement as can be seen from the *F* value (fit 17 in Table 2) and from the fit to the data (not shown). It did, however, refine close to a total CN of 2.4, which is consistent with the results from single-shell fits. For the oxidized sample, a single-shell fit gave a 1.96 Å Cu−O distance or a 1.99 Å Cu−N distance with a CN between 3 and 4 (minimum of 3.2). Comparison of single- and two-shell fits reveals that again the two-shell fit (fit 24 in Table 2) did not give a significant improvement.

The first-shell analysis of the data for the three samples thus clearly shows an increase in the CN by ∼1 when the reduced T1Hg Lc is reoxidized via the intermediate to the fully oxidized T1Hg Lc. It furthermore supports the edge results in that the first shell is split for the intermediate, an effect which might be caused by the presence of a 4-coordinate Cu(I) site, for which the average coordination distances would be expected to be longer than for a Cu(II) site.

The first-shell data of the intermediate were further examined to probe for the possible presence of a short Cu−O bond. A third shell of a shorter Cu−O distance was added with a fixed CN of 0.33 and a fixed distance starting at 1.70 Å which was then stepped to 1.85 Å with an interval of 0.05 Å. The fits were performed by varying the distances and DW factors of the two longer shells. In each case, a worse fit was obtained, with the newly added wave being out of phase with the other two waves. The DW factors for the longer bonds increased to compensate for the addition of this third wave. If the DW factor of the short Cu−O was allowed to vary, it refined to an unrealistically large value (fit 9 in Table 2). Also, when the short Cu−O distance was allowed to vary, it gave a refined value of 1.80 Å with a negative CN. These results clearly indicate that a short Cu−O bond is not present in the trinuclear center of the oxygen intermediate of T1Hg Lc.

Comparison of the FTs of the EXAFS spectra of the three T1Hg Lc samples in Figure 8 shows a striking difference at about 3.0 Å. While no major peaks are present in this region for the oxidized and the reduced data, a prominent peak is present in the FT of the data of the oxygen intermediate. The Fourier-backtransform of this peak gives an EXAFS signal with an amplitude envelope which peaks at high *k*, indicating a strong high-*Z* backscatterer (Figure 8, inset). The fit to the filtered data obtained by varying the distances and DW factors with a fixed CN of 0.67 gave a Cu−Cu distance of 3.39 Å and a rather low DW factor (fit 10 in Table 2). This calculated DW factor is in fact lower than the value extracted from the dihydroxy bridged binuclear cupric model, suggesting possibly a more rigid structure, and additional contribution from second-shell low-*Z* scatterers to this FT peak. A Cu−Cu distance of 3.39 Å, with a shortest distance to the bridging atom of 1.91 Å, would give a Cu−X−Cu angle of 125°. At such an angle a multiple-scattering contribution to this peak would be expected to be rather small. The level of contribution was, however, tested by calculating *ab initio* simulated single and multiple scattering EXAFS signals using the GNXAS methodology and software.[50,51] It was found that the multiple-scattering contribution at this angle was negligible, and that an angle of >160° would be required to give a significant enhancing effect on the FT magnitude, which corresponds to a Cu−Cu distance of >3.7 Å. The empirical fit matched the data quite well as seen in Figure 9, inset. Therefore, the pronounced outer-shell peak corresponding to a relatively short Cu−Cu distance with a low DW factor strongly suggests the presence of two Cu's bridged at ∼3.4 Å in the oxygen intermediate of T1Hg Lc.

(E) Absorption, CD, and MCD. (1) Ligand Field Region. The CD and MCD spectra in the ligand field region of the T1Hg Lc oxygen intermediate and that of fully oxidized T1Hg Lc obtained from the complete decay of the intermediate are shown in Figure 10. Under these conditions the intermediate sample has decayed to 20(±5)% fully oxidized T1Hg Lc; also the T1Hg Lc preparation contained about 5(±2)% Cu in the T1 site. These contributions including their error range have been subtracted from both the CD and MCD spectra of the intermediate and the resultant spectra were renormalized. The type 1 Cu contribution has also been subtracted from the CD and MCD spectra of the resting T1Hg Lc for comparison to the intermediate. The MCD spectrum of the T1Hg Lc oxygen intermediate (Figure 10B) shows no features in the ligand field region, within the error bar of the MCD experiment, indicating that there are *no paramagnetic Cu centers in the intermediate*. Comparing the MCD spectrum of the intermediate with that of the resting enzyme, the type 2 d−d features present in the resting protein at (+)850 nm, (−)720 nm, and (−)550 nm are absent in the intermediate, suggesting that the type 2 copper is reduced in the intermediate, in agreement with the results from EPR and SQUID magnetic susceptibility results. On decay of the intermediate, the type 2 d−d features reappear in the MCD correlating with the appearance of the type 2 EPR signal.

The CD spectrum of the intermediate appears similar to that of resting T1Hg Lc, but with systematic variations in the energy and intensity of the bands (Figure 10A). Since the MCD spectrum of the intermediate lacks any bands in the ligand field

(50) Filipponi, A.; Di Cicco, A.; Tyson, T. A.; Natoli, C. R. *Solid State Commun.* **1991**, *78*, 265.

(51) Westre, T. E.; Di Cicco, A.; Filipponi, A.; Natoli, C. R.; Hedman, B.; Solomon, E. I.; Hodgson, K. O. *J. Am. Chem. Soc.* **1995**, *117*, 1566.

Table 2. Summary of EXAFS Curve-Fitting Results for Intermediate, Reduced, and Oxidized T1Hg Laccase[a]

sample	fit no.	Fourier window, Å	element	CN[b]	distance, Å	c2[c]	*F*
intermediate	1	0.80−1.95	N	3.0	1.97	−0.023	0.34
	2	0.80−1.95	N	3.4	1.97	−0.025	0.33
	3	0.80−1.95	N	4.0	1.97	−0.028	0.35
	4	0.80−1.95	O	3.0	1.94	−0.025	0.24
	5	0.80−1.95	O	3.4	1.94	−0.027	0.23
	6	0.80−1.95	O	4.0	1.94	−0.030	0.25
	7	0.80−1.95	N	2.0	2.03	−0.024	0.19
			O	1.4	1.90	−0.018	
	8	0.80−1.95	N	1.3	2.06	−0.020	0.19
			O	2.0	1.91	−0.019	
	9	0.80−1.95	N	2.0	2.02	−0.028	0.19
			O	1.4	1.91	−0.018	
			O	0.33	1.75[d]	−0.332	
	10	2.70−3.40	Cu	0.67	3.39	−0.023	0.14
reduced	11	0.70−1.98	N	2.0	1.97	−0.022	0.30
	12	0.70−1.98	N	2.3	1.97	−0.024	0.29
	13	0.70−1.98	N	3.0	1.97	−0.029	0.31
	14	0.70−1.98	O	2.0	1.93	−0.024	0.25
	15	0.70−1.98	O	2.4	1.93	−0.027	0.24
	16	0.70−1.98	O	3.0	1.93	−0.031	0.27
	17	0.70−1.98	N	1.4	2.01	−0.025	0.24
			O	1.0	1.90	−0.020	
oxidized	18	0.80−1.90	N	3.0	1.99	−0.019	0.38
	19	0.80−1.90	N	3.2	1.99	−0.020	0.37
	20	0.80−1.90	N	4.0	1.99	−0.023	0.42
	21	0.80−1.90	O	3.0	1.96	−0.021	0.26
	22	0.80−1.90	O	3.2	1.96	−0.022	0.26
	23	0.80−1.90	O	4.0	1.96	−0.026	0.32
	24	0.80−1.90	N	1.3	2.06	−0.021	0.24
			O	2.0	1.94	−0.017	

[a] Errors are estimated to be about ±0.03 Å for distances and 25% for coordination numbers.[37−39] [b] CN = coordination number. [c] c2 is the amplitude parameter having the functional form of the DW factor, *i.e.*, $\exp(-2\sigma^2 k^2)$, where $c2 = -2\sigma^2$. A more negative value of c2 denotes a larger value of σ^2 and thus a more disordered structure. [d] Values fixed.

region, the CD bands in the intermediate must be associated with Cu(II)'s having a diamagnetic ground state and are assigned to the oxidized type 3 site. Thus both type 3 coppers are oxidized in the intermediate and antiferromagnetically coupled (consistent with SQUID magnetic susceptibility, *vide supra*), implying 2 electrons have been transferred to dioxygen, supporting its description as *a peroxide-level intermediate*. Our earlier work showed that the type 2 copper does not contribute significantly to the RT CD spectrum of T1Hg Lc.[6] The CD bands in resting T1Hg Lc are therefore assigned as d−d transitions of the type 3 copper centers. The differences in the CD spectra of resting T1Hg Lc and the intermediate must then be due to distortions of the oxidized type 3 site.

Gaussian resolution (see supporting information) reveals six bands for resting T1Hg Lc and five bands for the intermediate (the sixth band in resting T1Hg Lc appears as a low-energy tail and a small shift to lower energy would make it unobservable in this spectral region). Using ligand perturbations, the bands in resting T1Hg Lc have been assigned to two inequivalent type 3 coppers[6] (designed type 3_α and type 3_β, indicated in Figure 9). The inequivalence requires somewhat different ligand fields indicating different degrees of distortion. On going from the resting to the oxygen intermediate, the three higher energy bands due to type 3_α show a significant shift to higher energy, while the three lower energy bands due to type 3_β show minor perturbations in energy and significant changes in intensity.

The large shift of the bands associated with the type 3_α copper to higher energy in the intermediate indicates an increase in the energy of its $d_{x^2-y^2}$ orbital, which is consistent with peroxide binding in the equatorial plane of the type 3_α copper. The limited changes in the energies of the type 3_β bands and their change in intensity between resting and the oxygen intermediate of T1Hg Lc could result from distortions of this copper center on formation of the intermediate.

(2) Charge Transfer Region. (i) Absorption and CD. The absorption spectrum of the T1Hg Lc oxygen intermediate (with the spectrum of the fully oxidized protein subtracted, and the resultant renormalized) is shown in Figure 10A. It exhibits bands at 340 nm ($\epsilon = 5000\ M^{-1}\ cm^{-1}$) and 470 nm ($\epsilon = 1800\ M^{-1}\ cm^{-1}$) and a weak band at 670 nm. The lowest energy band is assigned as a Cu d−d transition while the higher energy bands are too high in energy to be ligand field transitions and are assigned as CT transitions due to the peroxo ligand of the intermediate (*vide supra*) since they are not found in resting T1Hg Lc. The higher energy, more intense band at 340 nm is assigned as $\pi^*_\sigma \rightarrow$ Cu(II) CT while the lower energy, weaker transition at 470 nm is assigned as $\pi^*_V \rightarrow$ Cu(II) consistent with assignments of analogous transitions in other peroxo−Cu(II) complexes.[52,53] EPR, SQUID magnetic susceptibility, and LT MCD studies in the ligand field region indicate that the type 2 copper is reduced in the intermediate, therefore, these peroxide CT transitions are to the copper(s) of the oxidized type 3 site.

EXAFS studies show two coppers bridged at a distance of 3.4 Å in the intermediate (*vide supra*). If the peroxide were bridging between two Cu(II)'s, then the CT absorption spectrum of the intermediate should be comparable to that of one of the two structurally characterized side-on (a close structural analog of oxyhemocyanin[54,55]) and *trans* end-on[56] (which is predicted

(52) Baldwin, M. J.; Root, D. E.; Pate, J. E.; Fujisawa, K.; Kitajima, N.; Solomon, E. I. *J. Am. Chem. Soc.* **1992**, *114*, 10421.
(53) Solomon, E. I.; Tuczek, F.; Root, D. E.; Brown, C. A. *Chem. Rev.* **1994**, *94*, 827.
(54) Kitajima, N.; Fujisawa, K.; Moro-oka, Y.; Toriumi, K. *J. Am. Chem. Soc.* **1989**, *111*, 8975.
(55) Kitajima, N.; Fujisawa, K.; Fujimoto, C.; Moro-oka, Y.; Hashimoto, S.; Kitagawa, T.; Toriumi, K.; Tatsumi, K.; Nakamura, A. *J. Am. Chem. Soc.* **1992**, *114*, 1277.

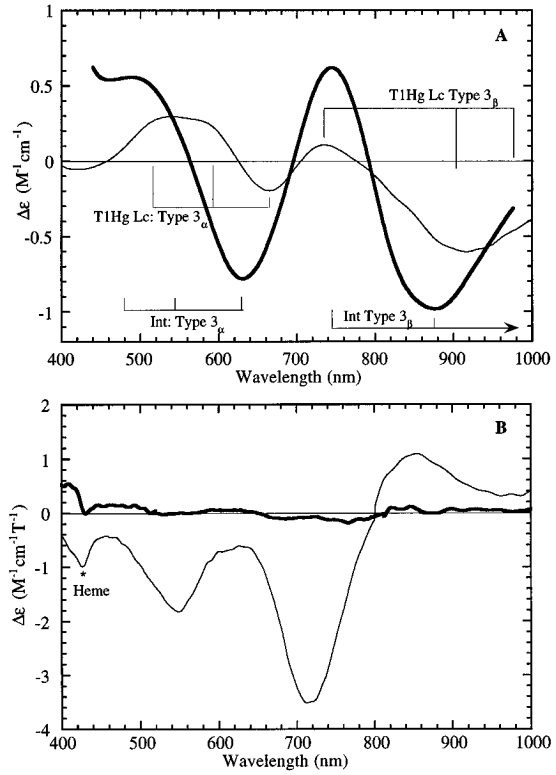

Figure 9. (A) 298 K CD and (B) 4.2 K MCD spectra of (light solid line) resting and (dark solid line) oxygen intermediate of T1Hg Lc. A 4(±2)% native Lc contaminant in the preparation has been subtracted from the CD and MCD spectra of the resting and intermediate forms. A 20(±5)% decayed, fully oxidized component has also been subtracted from the CD and MCD spectra of the intermediate. The spectra have been renormalized. The CD spectra are in units of M^{-1} cm^{-1} and the MCD spectra are in units of M^{-1} cm^{-1} T^{-1}. The brackets in the CD spectra indicate the positions of the bands associated with each Cu for both the resting and intermediate forms of T1Hg Lc.

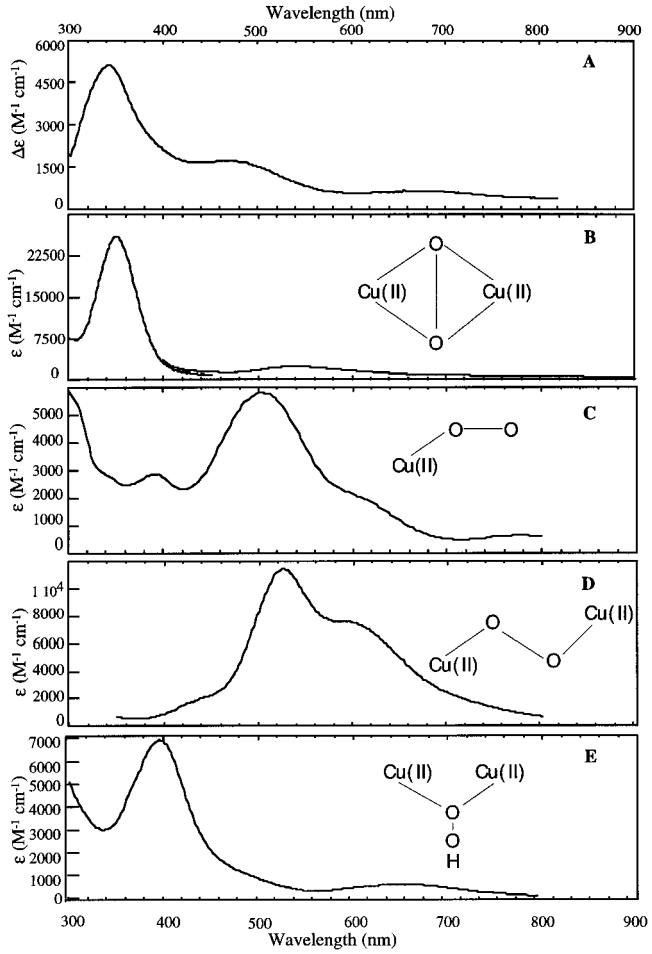

Figure 10. Absorption spectra of the T1Hg Lc oxygen intermediate along with peroxo Cu(II) model complexes: (A) CT absorption spectrum of T1Hg Lc intermediate from which the spectrum of the decayed fully oxidized protein has been subtracted and the spectrum normalized to 100% intermediate. The spectrum was obtained at room temperature in 0.1 M phosphate buffer pH 7.4. (B − E) Spectra of model complexes, with structural types indicated, reproduced from the references mentioned in the text.

to be similar to the *cis* end-on[57]) peroxide bridged binuclear cupric model complexes given in Figures 10B and 10D. Comparing the energy and intensity of the π^*_σ CT transition of the intermediate (at 340 nm) with that of the model complexes, the energy of the CT transition in the intermediate is similar to that of the side-on μ-η^2:η^2 peroxo cupric dimer (Figure 10B) model, but its intensity is 5-fold lower in the intermediate. Relative to the *trans* μ-1,2 cupric dimer (Figure 10D), the band in the intermediate is at much higher energy and also is much lower in intensity. π^*_σ CT intensity has been shown to reflect the strength of the σ donor interaction of peroxide with Cu(II) hence the number of peroxo O−Cu(II) bonds.[52,53] The lower intensity of the CT transition in the intermediate ($\epsilon = 5000$ M^{-1} cm^{-1}) compared to that of the side-on μ-η^2:η^2 peroxo cupric dimer (B) ($\epsilon = 25\,000$ M^{-1} cm^{-1}) and the *trans* μ-1,2 cupric dimer (D) ($\epsilon = 12\,000$ M^{-1} cm^{-1}) suggests a structure where peroxide is bound to only one Cu(II) in the intermediate.

Comparing the intermediate to a model complex where the peroxide is end-on bound to a single Cu(II)[58,59] (Figure 10C), the intensities of their π^*_σ CT transitions are comparable ($\epsilon =$ 5000 M^{-1} cm^{-1} in the intermediate vs $\epsilon = 5900$ M^{-1} cm^{-1} in the model complex) but the energy of the transition is much higher in the intermediate. While the comparable intensities in the two further support the description of only one peroxo O−Cu(II) bond in the intermediate, the much higher energy (~10 000 cm^{-1}) for the CT transition of the intermediate relative to that of the terminal peroxo cupric model complex is indicative of an additional bonding interaction in the intermediate which would lower the energy of the ligand donor orbital and thus increase the energy of the CT transition. This additional bonding interaction cannot be with another Cu(II) since this would increase the CT intensity which is not observed. A reasonable means to increase the bonding interaction of the peroxide is through its protonation which would lead to a stabilization of its π^*_σ orbital.[53]

Comparing the hydroperoxo bridged binuclear cupric model complex[60] (E) with the peroxo bridged cupric dimer (D) the π^*_σ CT transition is shifted ~6000 cm^{-1} to higher energy which is dominantly due to protonation of the peroxide. However, the π^*_σ CT transition in the intermediate is still ~4000 cm^{-1} higher in energy than the μ-1,1 hydroperoxo binuclear cupric dimer (E). The bridging interaction from EXAFS data combined with the CT intensity indicating a single hydroperoxide−Cu(II) bond suggests that the hydroperoxide bridges between

(56) Karlin, K. D.; Ghosh, P.; Cruse, R. W.; Farooq, A.; Gultneh, Y.; Jacobson, R. R.; Blackburn, N. J.; Strange, R. W.; Zubieta, J. *J. Am. Chem. Soc.* **1988**, *110*, 6769.
(57) Ross, P. K.; Solomon, E. I. *J. Am. Chem. Soc.* **1990**, *112*, 5871.
(58) Karlin, K. D.; Cruse, R. W.; Gultneh, Y.; Farooq, A.; Hayes, J. C.; Zubieta, J. *J. Am. Chem. Soc.* **1987**, *109*, 2668.
(59) Pate, J. E.; Cruse, R. W.; Karlin, K. D.; Solomon, E. I. *J. Am. Chem. Soc.* **1987**, *109*, 2624.
(60) Ghosh, P.; Tyeklar, Z.; Karlin, K. D.; Jacobson, R. R.; Zubieta, J. *J. Am. Chem. Soc.* **1987**, *109*, 6889.

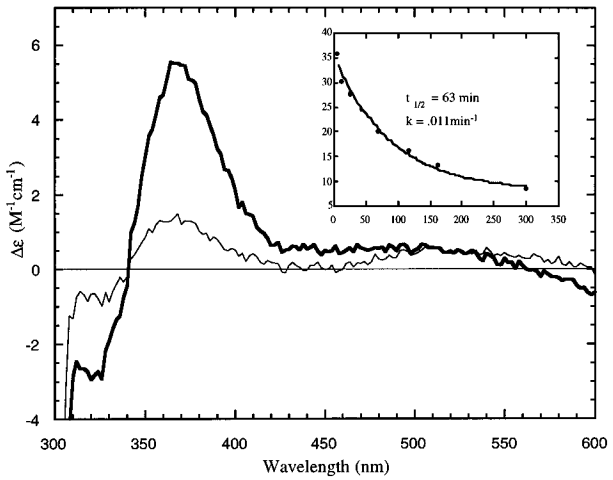

Figure 11. 298 K CD spectrum in the CT region of (dark solid line) T1Hg Lc intermediate and (light solid line) decayed, fully oxidized T1Hg Lc in 0.1 M phosphate buffer, pH 7.4. Inset shows kinetic profile for the decay of the 364-nm band.

one of the oxidized type 3 coppers and the reduced type 2 center. The alternative of associating the Cu···Cu interaction in the intermediate with the bridging hydroxide at the type 3 site is less likely since this interaction is not present in resting T1Hg Lc and hydroperoxide binding to one of the type 3 Cu(II)s would weaken its interaction with the hydroxide. (Note that a μ-1,1 hydroperoxo, μ-hydroxo type 3 dibridged structure is excluded both by the 3.4 Å Cu···Cu distance and low CT intensity.) μ-1,1 bridging of the hydroperoxide between a Cu(II) and a Cu(I) would further increase the CT energy relative to the μ-1,1 hydroperoxo bridged binuclear Cu(II) model complex in Figure 10E, as there would no longer be excited state antiferromagnetic coupling which lowers CT energies in bridged binuclear cupric dimers.[61] Thus μ-1,1 hydroperoxo bridging between one of the oxidized type 3 and the reduced type 2 seems the most reasonable structure for the intermediate based on its CT absorption spectrum combined with the EXAFS results.

The CD spectrum in the CT region of the intermediate at 298 K is shown in Figure 11. A positive band at 364 nm and a negative band at 320 nm are observed. Both features decrease in intensity with decay of the intermediate. The decrease intensity of the 364-nm band ($k \sim 0.011(\pm 0.001)$ min^{-1}, $t_{1/2} \sim 63(\pm 6)$ min, Figure 11 inset) correlates well with the decrease in intensity of the 340-nm absorption band ($k \sim 0.013(\pm 0.001)$ min^{-1}, $t_{1/2} \sim 53(\pm 4)$ min, see Figure 1). The energy of the CD bands does not correlate with that of any of the new absorption bands in the intermediate. They therefore do not appear to be associated with the $O_2^{2-} \rightarrow Cu^{2+}$ CT transitions of the intermediate. Similar bands (energies and intensities) are present in resting T1Hg Lc and have been assigned as ligand $\rightarrow$ Cu(II) CT transitions of the hydroxide bridge between the type 3 coppers[5] and the imidazole ligands at the type 3 center. The increase in intensity of these bands on formation of the intermediate would appear to reflect a perturbation of the type 3 center due to binding the hydroperoxo ligand at the trinuclear cluster.

(ii) MCD. The MCD spectrum in the CT region of the oxygen intermediate of T1Hg Lc (dark solid line) along with the fully decayed oxidized protein (light solid line) obtained at 5 T and 4.2 K is shown in Figure 12A. The intermediate shows bands at (+)364 and (−)318 nm which are temperature dependent indicating that they are associated with paramagnetic copper. Yet the intermediate was determined to be diamagnetic

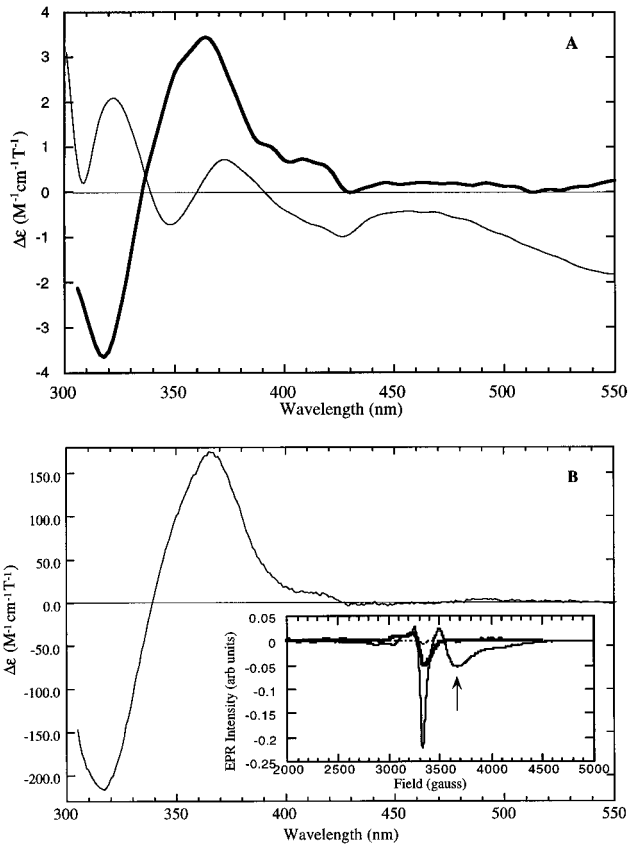

Figure 12. 4.2 K, 5 T MCD spectra of (A) (dark solid line) T1Hg Lc intermediate and (light solid line) decayed, fully oxidized T1Hg Lc in 0.1 M phosphate buffer, pH 7.4, 50% v/v glycerol. (B) Native laccase oxygen intermediate in 0.1 M phosphate buffer, pH 7.4, 50% v/v glycerol. (Under these conditions the sample contained 50% intermediate, the rest consisting primarily of unreacted reduced protein. The spectrum has been normalized to 100% intermediate to compare to the T1Hg Lc intermediate.) The inset shows X-band EPR spectra of (light solid line) native Lc intermediate, (dark solid line) T1Hg Lc intermediate, and (- - -) 2% of native Lc intermediate. The spectra have been normalized to the same gain, modulation, and protein concentration. Conditions: temperature 7 K, power 200 mW, modulation frequency 100 kHz, microwave frequency 9.517 GHz. The arrow indicates the characteristic feature of native intermediate in the high-field region. The signals in the $g = 2$ region are those due to a partially saturated type 2 copper (from the ∼30% decayed fully oxidized) in the T1Hg Lc intermediate sample and the oxidized type 1 site in the native intermediate sample.

by EPR, SQUID magnetic susceptibility, and ligand field MCD studies. Thus the MCD signals must correspond to a small percentage of paramagnetic copper which would not be detectable above the noise level in the above experiments (≤7%). The rate of decay of this MCD signal is found to be about the same as that of the T1Hg Lc intermediate in the 50% glycerol MCD sample ($t_{1/2}$ of ∼100 min). Comparison of this T1Hg Lc intermediate MCD spectrum with that of the native Lc oxygen intermediate[22] (Figures 12A and 12B) indicates that they are virtually identical, with the intensity of the T1Hg Lc intermediate signal being ∼2% of the native Lc intermediate signal. However, this signal cannot be due to the native contaminant present in the sample. The native intermediate (under the same 50% glycerol conditions as the T1Hg Lc intermediate MCD samples) has a $t_{1/2}$ of about 25 s[62] which is more than 200 times

(61) Tuczek, F.; Solomon, E. I. *Inorg. Chem.* **1993**, *32*, 2850.

(62) Sundaram, U.; Solomon, E. I. Unpublished results. Andréasson, L.-E.; Brändén, R.; Reinhammar, B. *Biochim. Biophys. Acta*. **1987**, *438*, 370.

faster than the decay of the T1Hg Lc intermediate ($t_{1/2}$ of ~100 min).

The strong similarity between the two MCD signals and the fact that the native laccase oxygen intermediate is at least one electron further reduced than the T1Hg Lc intermediate (due to the transfer of the additional electron from the type 1 site) suggests that the T1Hg Lc oxygen intermediate decays via electron transfer from the reduced type 2 (*vide supra*) to a species which closely resembles the native Lc oxygen intermediate. This intermediate, denoted T1Hg Lc−Int*, undergoes subsequent decay to fully oxidized T1Hg Lc. To explain the ~2% intensity and the observed decay rate of T1Hg Lc−Int*, the kinetic scheme in eq 6 was considered.

$$\text{T1Hg Lc−Int} \xrightarrow{k_1} \text{T1Hg Lc−Int*} \xrightarrow{k_2} \text{T1Hg Lc−Ox} \quad (6)$$

k is the rate of decay of the T1Hg Lc oxygen intermediate and k_2 the rate of decay of T1Hg Lc−Int*. The concentration of T1Hg Lc−Int* is then given by eq 7.[63]

$$[\text{T1Hg Lc−Int*}] = \frac{k_1(1 - e^{(k_1 - k_2)t})}{(k_2 - k_1)}[\text{T1Hg Lc−Int}] \quad (7)$$

The rate of decay of the T1Hg Lc intermediate (k_1) is 0.013 min^{-1}, and that of the T1Hg Lc−Int* species (k_2) is taken to be the same as the decay of the native intermediate (2.08 min^{-1}).[64] At $k_2 \gg k_1$ and $t > k_2$, the expression for [T1Hg Lc−Int*] simplifies to eq 8.

$$[\text{T1Hg Lc−Int*}] = \frac{k_1}{k_2}[\text{T1Hg Lc−Int}] \quad (8)$$

This gives a concentration of the T1Hg Lc−Int* species which is 0.6% of the T1Hg Lc intermediate.

The amount of [T1Hg Lc−Int*] expected to be present, based on rate constants of the two species, is in reasonable agreement with the ~2% observed by MCD, with the limited difference likely due to errors in the estimation of the $\Delta\epsilon$ of the native intermediates and the use of the native $\Delta\epsilon$ for the T1Hg−Int* species. Since the rate of decay of T1Hg Lc intermediate is much slower than that of T1Hg Lc−Int*, the decay of T1Hg Lc−Int* will be governed by the rate of decay of T1Hg Lc intermediate, which also explains the observation that the MCD signal in the CT region decays with the same rate as that of the T1Hg Lc oxygen intermediate.

The native intermediate exhibits a characteristic broad EPR signal at liquid He temperatures, with a high-field feature around 3700 G[20,47] (inset in Figure 12B). Comparison of the liquid He EPR spectrum obtained for the T1Hg Lc intermediate to that of the native intermediate scaled down to 2% (which is the amount of T1Hg Lc−Int* estimated to be present in the T1Hg Lc intermediate samples based on the MCD intensity) indicates that the native intermediate EPR signal, expected for the T1Hg Lc Int* species based on the MCD similarity, would not be discernible in the liquid He EPR spectrum of the T1Hg Lc intermediate above the noise level of the data.

Discussion

In our earlier studies, we defined the presence of an oxygen intermediate in T1Hg Lc, determined its relevance to oxygen reduction by the native enzyme, and presented some preliminary spectral characterization.[26] We have now performed a variety of detailed spectral studies which have defined key structural features of this intermediate. (i) This is a peroxide-bound intermediate. X-ray edge and ligand field CD/MCD data have shown that two coppers are oxidized in the intermediate, SQUID magnetic susceptibility studies have shown it to be diamagnetic, IRMS has shown that both O atoms of dioxygen are bound in the intermediate, and EXAFS has excluded the presence of a very short Cu−oxo bond. (ii) The two electrons are transferred to the dioxygen from both coppers of the type 3 center with the type 2 remaining reduced. This derives from CD in the d−d region which shows LF transitions due to both type 3 coppers requiring that both type 3 coppers are oxidized, and EPR and MCD in the d−d region which show no oxidized type 2 features. (iii) The type 3 Cu(II)'s in the intermediate are antiferromagnetically coupled indicating that they are bridged in the intermediate. The antiferromagnetism is required by both the SQUID magnetic susceptibility data ($-2J > 200$ cm^{-1}) and the presence of d−d bands in the CD spectrum having no corresponding LT (i.e., paramagnetic) MCD signal. The bridge between the type 3 coppers can be hydroxide as in the resting enzyme, the peroxide, or both. The dibridged possibility, however, is excluded by EXAFS data which show a Cu···Cu distance of 3.4 Å which is too long to accommodate two single atom bridges yet the CT spectrum would require that the peroxide bind as a μ-1,1 hydroperoxide. (iv) The peroxide in the intermediate binds to only one Cu(II) of the type 3 center. This derives from the relatively low intensity ($\epsilon \sim 5000$ M^{-1} cm^{-1}) of the peroxide $\pi^*_\sigma \rightarrow$ Cu(II) $d_{x^2-y^2}$ CT transition indicating that there can be only one σ donor bonding interaction with a Cu(II). This is also supported by the CD data in the d−d region showing that the LF transitions of only one Cu(II) (the type 3 Cu_α) are significantly perturbed by peroxide coordination in the intermediate. Thus the peroxide does not bridge between the two oxidized type 3 coppers and the antiferromagnetism of the type 3 site in the intermediate derives from an endogenous bridging hydroxide. (v) The peroxide does however bridge two coppers of the trinuclear copper site. This is demonstrated by the appearance of a strong outer-shell Cu−Cu peak at 3.4 Å in the EXAFS spectrum. Such a distinctive feature requires a small pair-wise Debye−Waller factor hence a bridging ligand having a strong bonding interaction with the two coppers. A similar interaction has previously been observed by EXAFS in Molluscan oxyhemocyanin from *Megathura crenulata*.[65] The interaction seen in the oxygen intermediate of T1Hg Lc cannot be associated with the hydroxide bridge between the type 3 copper pair as this Cu−Cu feature does not show up distinctly in the Fourier transform of the EXAFS of resting T1Hg Lc and coordination of peroxide to one of the type 3 Cu(II) center would decrease, not increase, its bonding interaction with the hydroxide bridge. Hence the peroxide of the intermediate appears to bridge between the type 3_α Cu(II) and the reduced type 2 copper center. Peroxide binding to the reduced type 2 copper center in the intermediate is also supported by the edge data and EXAFS (first shell) data which are most consistent with the reduced copper being four coordinate. Finally, the CT absorption spectrum of the intermediate indicates the presence of a strong σ donor bonding interaction of the peroxide which does not contribute CT intensity. This could in part be associated with bonding of the reduced type 2 center. However, the spectral correlation with peroxide−Cu(II) model complexes supports a μ-1,1 hydroperoxide description for this intermediate. These studies thus

(63) Atkins, P. W. *Physical Chemistry*, 4th ed.; W. H. Freeman and Company: New York, 1990; p 798.

(64) Andréasson, L.-E.; Brändén, R.; Reinhammar, B. *Biochim. Biophys. Acta* **1976**, *438*, 370.

(65) Co, M. S.; Hodgson, K. O.; Eccles, T. K.; Lontie, R. *J. Am. Chem. Soc.* **1981**, *103*, 984.

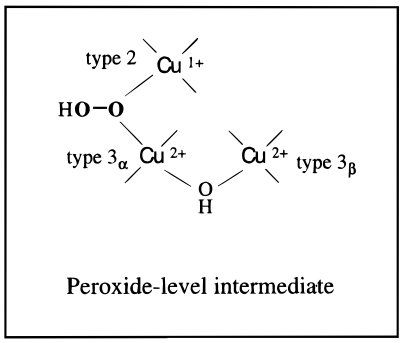

Figure 13. Spectroscopically effective model for the peroxide intermediate of T1Hg Lc.

provide strong support for the spectroscopically effective model for the peroxide-level intermediate[26] in the multicopper oxidases shown in Figure 13.

This model is different from that recently proposed[16] which is derived from an X-ray structural determination of the peroxide adduct of ascorbate oxidase. In the peroxide adduct structure, peroxide binds as hydroperoxide to one of the type 3 coppers but all bridging is eliminated and the Cu···Cu distances between the coppers in the trinuclear cluster are 4.8, 4.5, and 3.7 Å. This adduct structure (prepared by addition of peroxide to the oxidized protein) cannot be correct for the peroxide intermediate of T1Hg Lc (prepared by addition of dioxygen to the reduced protein) based on the above spectral data for the T1Hg Lc oxygen intermediate. If there were no ligands bridging the coppers of the trinuclear site in the peroxide intermediate, the two copper(II)'s would be paramagnetic. Yet the peroxide intermediate exhibits no EPR signal (down to liquid He temperatures and high powers), has no LT MCD signal in the ligand field region which would be present for paramagnetic Cu(II)'s, and is diamagnetic by SQUID magnetic susceptibility. Further, EXAFS data clearly show that two coppers in the intermediate are bridged at a distance of 3.4 Å.

Elimination of the extra electron associated with the type 1 copper has enabled us to obtain a peroxide intermediate in T1Hg Lc which decays slowly and therefore can be studied in detail to obtain mechanistic insight. The rate of decay of the peroxide intermediate is six orders of magnitude higher in its protonated form. This protonation appears to involve a residue in the vicinity of the trinuclear site with a pK_a of 5.2 which from crystal structure of ascorbate oxidase[9] appears to be the aspartate residue (ASP 73). This residue lies between the type 2 and type 3 centers of the trinuclear cluster and its carboxylate oxygen is at reasonable hydrogen bonding distance from the peroxide ligand of the oxygen intermediate.

The rate of decay of the protonated intermediate is still slow ($k = 0.6$ min^{-1}). Therefore protonation is not the rate-limiting step in the decay of the peroxide intermediate. Since this decay involves reduction of the peroxide by the type 2 copper this electron transfer process must then be very slow. From Marcus theory[66] three factors can influence this rate—driving force, electronic coupling matrix element, and Frank−Condon barrier. There is a reasonable pathway for electron transfer due to the peroxide bridging between the type 2 and type 3 copper centers (see Figure 13). However, the driving force of one-electron transfer from the type 2 copper (potential ~0.37 V[17]) to the peroxide ligand ($E°$ of $H_2O_2 + H^+ + e^- \rightarrow {}^\bullet OH + H_2O$ is 0.38 V vs NHE at pH 7.0)[67] is very low and the slow rate of electron transfer could then be due to a large Frank−Condon factor for

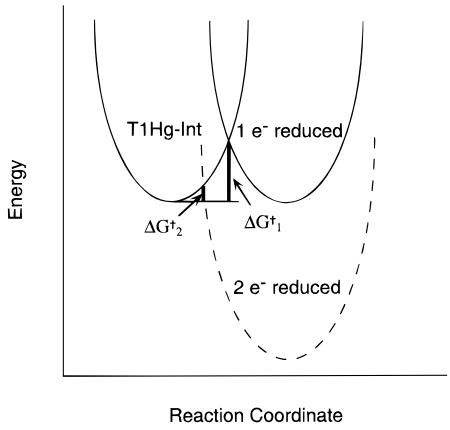

Figure 14. Potential energy diagram of reduction of peroxide in the intermediate of laccase: (—) 1-electron reduction; (- - -) 2-electron reduction. $\Delta G^\dagger_1$ and $\Delta G^\dagger_2$ are the activation energy barriers for 1- and 2-electron reduction, respectively.

reduction of the peroxide by the type 2 copper. While the geometry change with redox at the type 2 copper will certainly contribute, the dominant factor in this large Frank−Condon barrier is likely the distortion associated with O−O bond cleavage on reduction. This leads to the potential energy surface description for the decay of the peroxide intermediate shown in Figure 14 where the surface on the left is that of the intermediate and the solid surface on the right is that associated with one-electron transfer leading to cleavage of the O−O bond. From Figure 14 it is observed that a large distortion leads to a large thermal barrier ($\Delta G_1^\dagger$) for electron transfer for a moderate reduction potential. Alternatively, the rate of reduction of the putative peroxide intermediate in the native enzyme must be very fast. This derives from the fact that the rate of formation of the native intermediate and that of the T1Hg Lc intermediate are the same (2×10^6 M^{-1} s^{-1})[26] yet the native intermediate is best described as a 4-electron reduced hydroxide product species. Therefore the rate of reduction of the putative peroxide intermediate in the native enzyme must be much faster than its formation. The $>10^7$ increased rate of decay (i.e., 2-electron reduction) of the putative peroxide intermediate in native[26] ($k > 10^3$ s^{-1}) relative to the peroxide intermediate in T1Hg Lc ($k = 2.1 \times 10^{-4}$ s^{-1}) can be explained by the large difference in reduction potential between 2 and 1 electron reduction of peroxide ($E°$ of $H_2O_2 + 2H^+ + 2e^- \rightarrow 2H_2O$ is 1.35 V vs NHE at pH 7.0). This large increase in thermodynamic driving force leads to a much lower thermal barrier ($\Delta G_2^\dagger$) for electron transfer to a peroxide intermediate in the native enzyme for a reorganization energy comparable to that associated with reduction of the peroxide intermediate in T1Hg Lc (dashed curve in Figure 14 right).

The mechanistic importance of the T1Hg Lc peroxide intermediate to oxygen reduction by the native enzyme is emphasized by the facts that the T1Hg Lc peroxide intermediate decays to a form (denoted by T1Hg Lc−Int*) equivalent to the oxygen intermediate of the native enzyme (i.e., same MCD spectral features) and that both the T1Hg Lc intermediate and the native intermediate have the same rates of formation. The native intermediate had been described as a 3-electron reduced (from the type 1 and type 3 centers with the type 2 remaining reduced) hydroxyl radical[20,47] bound to the site. However, our MCD studies on this intermediate indicated that the $S = {}^1/_2$ observed must have significant Cu(II) character[22] indicating that the native intermediate would in fact be a 4-electron reduced hydroxide species bound to the trinuclear cluster with the type 2 oxidized. The decay of the T1Hg Lc intermediate likely involves reduction of the peroxide by oxidation of the type 2

(66) Marcus, R. A.; Sutin, N. *Biochim. Biophys. Acta* **1985**, *811*, 265.
(67) Sawyer, D. T. *Oxygen Chemistry*; Oxford University Press: New York, 1991.

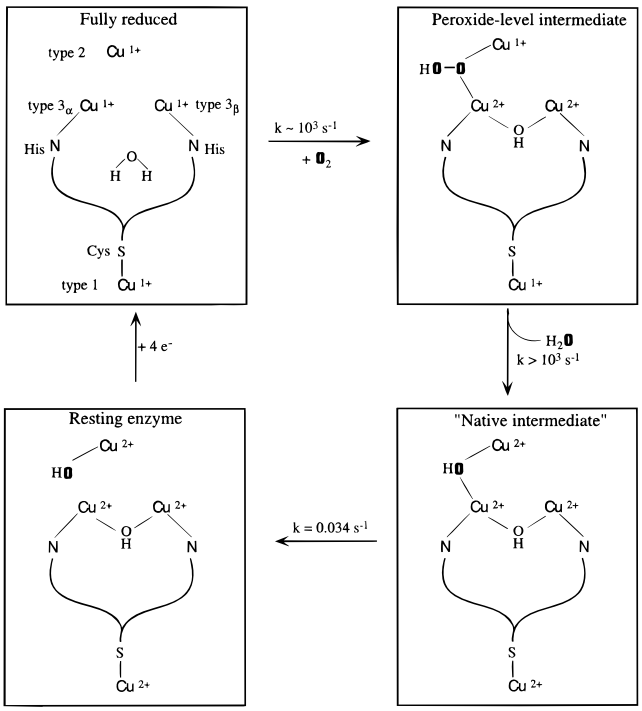

Figure 15. Proposed reaction mechanism of dioxygen reduction in the multicopper oxidases.

copper to produce OH^- bound to the site (releasing $^{\bullet}OH$ into the solution). Since the native intermediate involves either a type 2 Cu(I) + $^{\bullet}OH$ or type 2 Cu(II) + OH^- species and since both T1Hg Lc−Int* and native intermediate have the same spectral features, an internally consistent description of the native intermediate is hydroxide bound to a fully oxidized trinuclear cluster in support of the MCD results.

The above results lead to the mechanism of oxygen reduction to water by the multicopper oxidases shown in Figure 15. Initial reduction by 2 electrons from the type 3 center produces the peroxide intermediate studied in this paper where the peroxide bridges between the type 2 and type 3 centers (note that there is a H_2O molecule present between the two type 3 coppers, at ∼3.8 Å from one of the type 3 coppers and at ∼5 Å from the other type 3 copper in the crystal structure of fully reduced ascorbate oxidase,[16] which could produce the hydroxide bridge at the oxidized type 3 site). This structural model provides insight into the requirement of the type 2 Cu for dioxygen reduction. The peroxide intermediate undergoes further reduction which is rapid in the native enzyme because it involves 2 electrons (from type 1 and type 2 centers) providing a large thermodynamic driving force to overcome the significant Frank−Condon barrier associated with O−O bond cleavage. This produces the hydroxide bridged product (i.e., the "native intermediate" shown in Figure 15), which subsequently decays by cleavage of the type 3 Cu(II)−OH bond to the resting native enzyme. Note from Figure 15 that the hydroxide bridge at the type 3 center would not derive from O_2, which is consistent with the fact that reduction of $^{17}O_2$ by native laccase results in $^{17}OH^-$ or $H_2{}^{17}O$ bound to the type 2 copper in the reoxidized resting enzyme.[19,20]

Finally it is important to emphasize that the geometric and electronic structure of the peroxide intermediate in laccase is fundamentally different from that in the coupled binuclear copper proteins hemocyanin and tyrosinase which would contribute to differences in function. Hemocyanin and tyrosinase are involved in the reversible binding and activation of dioxygen for hydroxylation chemistry, respectively. Both involve a peroxide intermediate with the μ-η^2:η^2 bridging structure and characteristic spectral features shown in Figure 10B. The unique electronic structure of the hemocyanin/tyrosinase peroxide intermediate has been studied in some detail[52] and shown to make a significant contribution to the reversible binding and activation of peroxide. Studies are now underway to understand the electronic structure of the peroxide intermediate in the multicopper oxidases (Figure 13) and define its contribution to the irreversible binding of peroxide at the trinuclear site and promotion of its further reduction to water.

Acknowledgment. We are grateful to the National Institutes of Health (Grant DK31450 to E.I.S. and Grant RR-01209 to K.O.H.) and the National Science Foundation (Grant CHE-9423181 to K.O.H.) for support of this work. The SSRL is supported by the Department of Energy, Office of Basic Energy Sciences, Divisions of Chemical and Materials Sciences, and in part by the NIH, National Center for Research Resources, Biomedical Research Technology Program, and by DOE's Office of Health and Environmental Research. We gratefully acknowledge Dr. Carol Kendall and Mr. Doug White of United State Geological Survey in Menlo Park for the IRMS measurements. We thank David E. Root for helpful discussions and Dr. Martin L. Kirk for assistance with the SQUID magnetometer. W.S. thanks Sogang University, Seoul, Korea, for allowing a two month leave of absence to finalize this paper.

Supporting Information Available: Gaussian fits and fitting parameters of ligand field CD spectra shown in Figure 9A (2 pages). This material is contained in many libraries on microfiche, immediately follows this article in the microfilm version of the journal, can be ordered from the ACS, and can be downloaded from the Internet; see any current masthead page for ordering information and Internet access information.

JA953621E